ACS Catalysis

Research Article

pubs.acs.org/acscatalysis

Mechanism of *N,N,N*-Amide Ruthenium(II) Hydride Mediated Acceptorless Alcohol Dehydrogenation: Inner-Sphere β-H Elimination versus Outer-Sphere Bifunctional Metal–Ligand Cooperativity

Kuei-Nin T. Tseng, Jeff W. Kampf, and Nathaniel K. Szymczak*

Department of Chemistry, University of Michigan, Ann Arbor, Michigan 48109, United States

Supporting Information

ABSTRACT: The reversible transformations between ketones and alcohols via sequential hydrogenation–dehydrogenation reactions are efficiently achieved using a single precatalyst HRu(bMepi)$(PPh_3)_2$ (bMepi = 1,3-bis(6′-methyl-2′-pyridylimino)isoindolate). The catalytic mechanism of HRu(bMepi)$(PPh_3)_2$ mediated acceptorless alcohol dehydrogenation (AAD) has been investigated by a series of kinetic and isotopic labeling studies, isolation of intermediates, and evaluation of Ru(b4Rpi)$(PPh_3)_2$Cl (R = H, Me, Cl, OMe, OH) complexes. Two limiting dehydrogenation scenarios are interrogated: inner-sphere β-H elimination and outer-sphere bifunctional double hydrogen transfer. Isotopic labeling experiments demonstrated that the proton and hydride transfer in a stepwise manner. Catalyst modifications suggest that the imine group on the bMepi pincer scaffold is not necessary for catalytic alcohol dehydrogenation. Evaluation of the kinetic experiments and catalyst modifications suggests a pathway whereby HRu(bMepi)$(PPh_3)_2$ operates via the inner-sphere β-H elimination mechanism. Following a single PPh_3 dissociation, an alcohol substrate can bind and undergo proton transfer followed by a turnover-limiting β-H elimination step. Analysis of the Eyring plot established activation parameters for the β-H elimination reaction as $\Delta H^{\ddagger}$ = 15(1) kcal/mol and $\Delta S^{\ddagger}$ = −41(3) eu. AAD reactions using a series of Ru(b4Rpi)$(PPh_3)_2$Cl complexes indicated that the *ortho*-substituted methyl groups of bMepi slightly impede catalytic activity, and electronic modifications of the pincer scaffold have a minimal effect on the reaction rate.

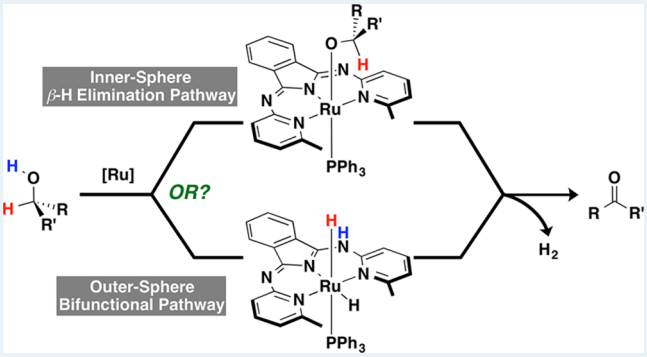

KEYWORDS: *acceptorless alcohol dehydrogenation, ruthenium, ligand effects, inner-sphere mechanism, outer-sphere mechanism, metal–ligand cooperativity*

INTRODUCTION

Transition-metal-catalyzed acceptorless alcohol dehydrogenation (AAD) with the liberation of H_2 is an atom-economical and selective route to generate a variety of organic carbonyl synthons.[1] In the context of the "hydrogen energy economy", AAD also provides a highly desirable strategy for promoting H_2 release from suitable biomass feedstocks for chemical energy storage applications.[2]

To achieve high atom economy (no exogenous additives), promoterless AAD reactions are most often mediated by bifunctional catalysts that operate via a metal–ligand cooperative mechanism. This ligand-assisted, transition-metal-catalyzed process differs from the classical inner-sphere mechanism by not requiring coordination of the substrate, thus enabling outer-sphere proton transfer to a ligand-based basic site with concurrent hydride transfer to the metal center (Scheme 1).[3] For example, Milstein's group developed a series of pyridyl PNE (E = PR_2 or NR_2) Ru pincer complexes (**1**, HRu(PNE)(CO)) that employ cooperation of the metal center with the ligand via aromatization–dearomatization of the central pyridinyl group concomitant with protonation–deprotonation of the methylene arm (Scheme 2, left panel).[1a,4]

Computational studies revealed that **1** favors an outer-sphere bifunctional double hydrogen-transfer pathway rather than an inner-sphere β-H elimination process.[5] More recently, a computational study by Yamaguchi, Fujita, and co-workers demonstrated that the AAD reaction of benzyl alcohol catalyzed by Cp*Ir(bpyO)(**2**, bpyO = α,α'-bipyridonate) also operates via an outer-sphere pathway, where the metal center and the bipyridonate motif work synergistically to oxidize benzyl alcohol en route to H_2 elimination with the aid of an alcohol bridge (Scheme 2, right panel).[6] Collectively, these and related studies establish the importance of a cooperative mechanism to achieve efficient dehydrogenation activity.

Received: May 6, 2015
Revised: August 4, 2015

DOI: 10.1021/acscatal.5b00952
ACS Catal. 2015, 5, 5468–5485

Scheme 1. Generalized Catalytic Cycles for the Inner-Sphere and Outer-Sphere Dehydrogenation Pathways

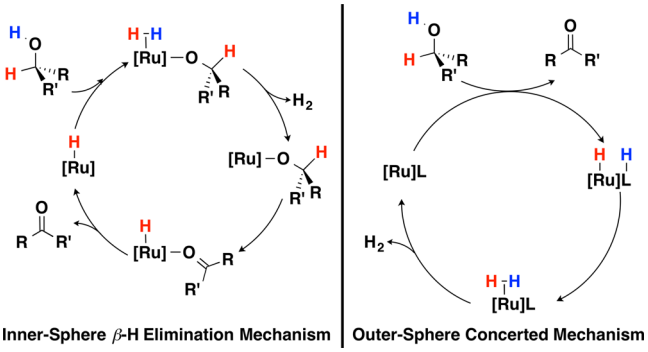

However, in systems that contain bifunctional groups, it may be ambiguous whether a cooperative pathway is actually required for efficient dehydrogenation.[7]

We recently reported an *N,N,N*-bMepi (bMepi =1,3-bis(6′-methyl-2′-pyridylimino)isoindolate) Ru^{II} hydride complex (**3**, $HRu(bMepi)(PPh_3)_2$) capable of catalyzing promoterless and chemoselective AAD reactions.[8,9] Of particular note, precatalyst **3** promotes acceptorless dehydrogenation of secondary alcohols to ketones, acceptorless dehydrogenative coupling of primary alcohols to esters, and diols to lactone products with high conversion efficiencies. Importantly, neither of these reactions requires exogenous base or hydrogen acceptor additives, and the catalyst system is unusually selective for the dehydrogenation of secondary alcohols in the presence of primary alcohols. Preliminary analysis of the alcohol dehydrogenation reaction revealed two key findings: (1) a homogeneous active catalyst, as assessed by mercury and substoichiometric ligand poisoning experiments, and (2) the release of PPh_3 under catalytic conditions. In this article, we use these observations as an entry point to disclose a detailed mechanistic analysis of a series of kinetic rate data including isotopic labeling studies, stoichiometric reactions to probe catalytic intermediate species, and new ligand variants to understand the steric and electronic effects of the bMepi pincer ligand on the activity of the Ru complex. We aim to answer the following key questions: (1) Does precatalyst **3** participate in an inner- or outer-sphere dehydrogenation pathway? (2) What are the details of the intermediates in the dehydrogenation catalytic cycle? (3) What impact do the steric (*ortho*-substituted methyl groups) and electronic (electron donating and withdrawing groups in the secondary coordination sphere) profiles of the bMepi pincer ligand have on alcohol dehydrogenation?

RESULTS AND DISCUSSION

Limiting Mechanistic Scenarios for AAD Catalyzed by 3.

Based on prior PPh_3 studies[8] and the observation of a first-order dependence of the rate of 1-phenylethanol (1PhEtOH) dehydrogenation on [**3**],[10] two limiting monometallic alcohol dehydrogenation pathways mediated by **3** are proposed in Scheme 3. For either pathway, phosphine dissociation from **3**

Scheme 3. Proposed Inner-Sphere and Outer-Sphere Dehydrogenation Pathways

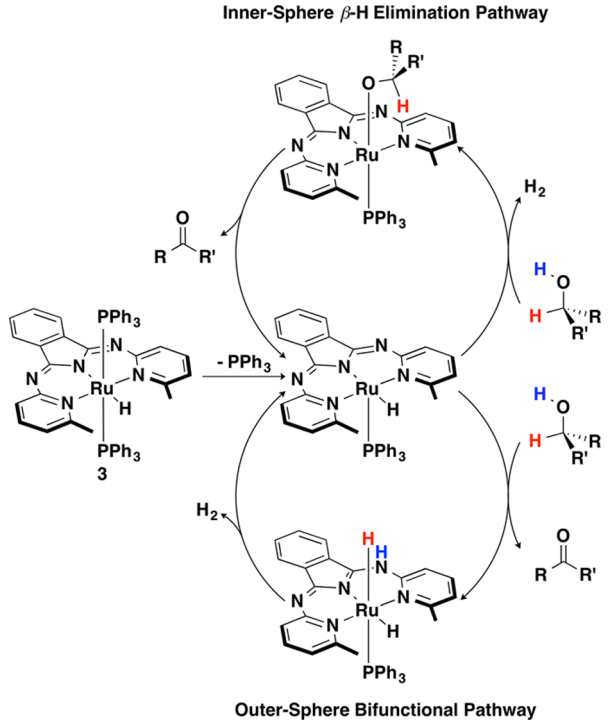

Scheme 2. Proposed AAD Reaction Pathway Mediated by 1 and 2

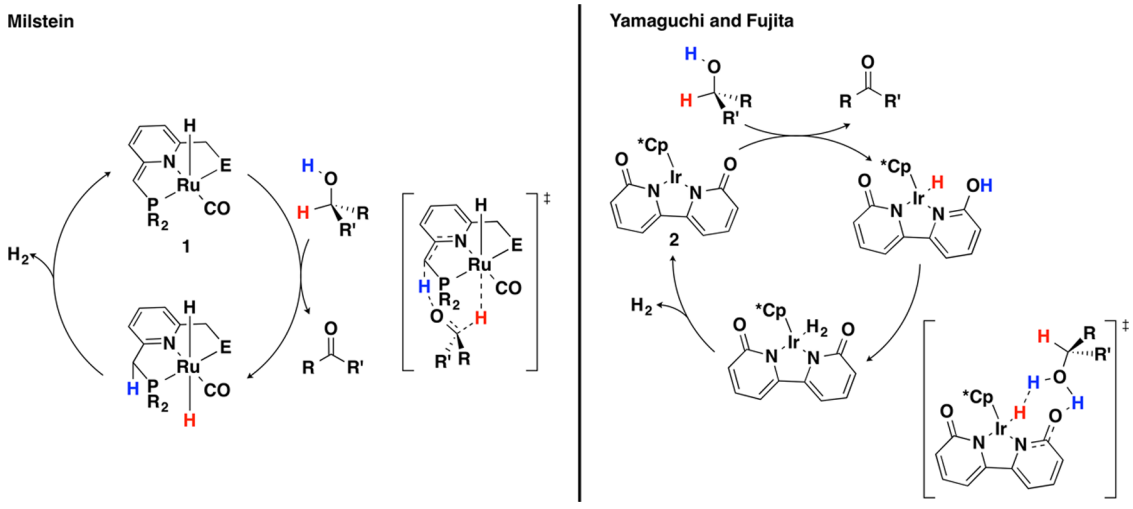

DOI: 10.1021/acscatal.5b00952
ACS Catal. 2015, 5, 5468−5485

generates a coordinately unsaturated Ru species that is able to participate in either an inner-sphere β-H elimination pathway (Scheme 3, top panel) or an outer-sphere concerted pathway (Scheme 3, bottom panel). In the inner-sphere cycle, proton transfer from the alcohol to the Ru hydride affords a Ru-alkoxide species (likely via a transient Ru-H_2 intermediate), which undergoes β-H elimination to complete the cycle. An alternative pathway to the inner-sphere β-H elimination mechanism is the outer-sphere pathway, where both proton and hydride transfer occur without requiring coordination to Ru. Complex **3** operating via this pathway may involve proton transfer to the imine (or isoindolate) group on the bMepi-ligand backbone with concurrent hydride transfer to the Ru-metal center. Both of these AAD mechanistic scenarios are evaluated by a series of kinetic experiments, catalyst modifications, as well as isolation of proposed intermediates.

Standard Conditions for Kinetic Studies. In order to examine the operative pathway for catalysis by **3**, 1PhEtOH was selected as a standard substrate because its low volatility permits heating in an open system. Additionally, the reverse reaction, reduction of acetophenone to 1PhEtOH, is generally accepted as a standard test for (transfer) hydrogenation catalysis.[3,11] The dehydrogenation reaction was performed in an open system inside an inert-atmosphere glovebox, and the conversion of 1PhEtOH to acetophenone was monitored by ^{1}H NMR spectroscopy using phenyltrimethylsilane (PhTMS) as an internal standard (Scheme 4). The observed reaction rates were

Scheme 4. Standard Reaction Conditions of AAD of 1PhEtOH Catalyzed by 3

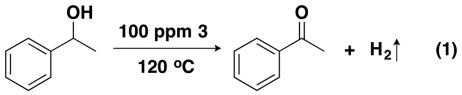

Standard Conditions:
[3] = 7.4 x 10-4 M
[1PhEtOH] = 7.5 M
[PhTMS] = 0.53 M

obtained using the method of initial rates. All kinetic experiments were simultaneously performed in triplicate. Standard reaction conditions for kinetic studies employed a vial containing 7.5 M 1PhEtOH and 0.01 mol % **3**. After the reaction mixture was heated to 120 °C for 4 h, acetophenone was observed in 11.6% conversion, which corresponds to an initial rate of $5.2(2) \times 10^{-5}$ M·s^{-1}, a turnover number (TON) of 1213, and a turnover frequency (TOF) of 303 h^{-1}. To establish confidence in the method of initial rates in this system, a reaction rate of 5.8×10^{-5} M·s^{-1} (within 10% error of the initial rate) at 4 h was obtained from the first derivative of an exponential fit of the complete dehydrogenation reaction profile (see Figure S2).

Triphenylphosphine Dependence. Based on our prior studies that showed free PPh_3 during catalysis, the dependence on PPh_3 concentration was examined to determine whether PPh_3 dissociation contributed to a turnover-limiting step in either of the proposed alcohol dehydrogenation cycles. The order in [PPh_3] was determined by measuring the observed rates for 1PhEtOH dehydrogenation over several PPh_3 concentrations under the reaction conditions listed in Scheme 4. No dependence on the rate of 1PhEtOH dehydrogenation was observed up to 20 equiv of PPh_3 (14.5 mM) relative to **3** (Figure 1).

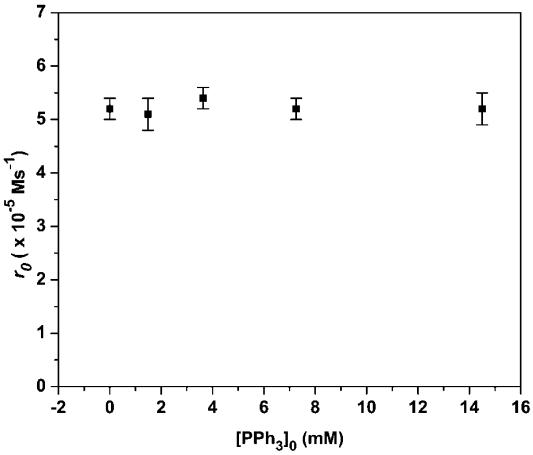

Figure 1. Influence of [PPh_3] on the reaction rates for 1PhEtOH dehydrogenation catalyzed by **3**.

The zero-order [PPh_3] dependence (up to 20 equiv) suggests that PPh_3 dissociation from **3** is not included in the turnover-limiting step and furthermore that phosphine binding/release is not in an equilibrium with the turnover-limiting step under these conditions. Therefore, the turnover-limiting step must be either β-H elimination (inner-sphere) or H_2 formation reaction (outer-sphere). Alternatively, for this to be true for a proton/hydrogen-transfer turnover-limiting step, the alcohol binding would have to be irreversible, which is highly improbable.[12]

1-Phenylethanol Dependence. In both the inner- and outer-sphere dehydrogenation scenarios (Scheme 3), the next step following PPh_3 dissociation involves the alcohol substrate. A rate dependence on [1PhEtOH] would be anticipated if the turnover-limiting step was alcohol binding followed by deprotonation (inner-sphere) or proton and hydride transfer from the alcohol (outer-sphere). The influence of 1PhEtOH concentration on the catalytic rate was examined by changing the [1PhEtOH] while holding the initial concentration of **3** constant. Over the range of 6.5−8 M 1PhEtOH, the observed reaction rate profile displayed a linear dependence on [1PhEtOH] from 6.5 to 7.5 M 1PhEtOH, then the rate reached culmination after 7.5 M 1PhEtOH with an averaged catalytic rate of $5.2(2) \times 10^{-5}$ M·s^{-1} (Figure 2).[13] The reaction rate dependence on [1PhEtOH] suggests a pre-equilibrium model in which at high [1PhEtOH] the equilibrium is driven to the right, and the dependence on [1PhEtOH] drops from the rate law. This model could fit either the inner- or outer-sphere pathways, where a pre-equilibrium alcohol binding and proton/hydrogen transfer is followed by a slow metal-based reaction (e.g., β-H elimination or H_2 formation). Given that two different mechanistic regimes exist at high and low [1PhEtOH], it is important to note that the kinetic experiments were performed at an initial [1PhEtOH] of 7.5 M (Scheme 4, unless otherwise stated), and under these conditions, the catalyst operated in the linear regime when the reaction proceeded 10−15%.

Temperature Dependence. The activation parameters for 1PhEtOH dehydrogenation mediated by **3** at low and high [1PhEtOH] were analyzed to interrogate the transition-state structures. The reaction rates were measured over a 40 °C temperature range and plotted according to an Eyring analysis (Figure 3). In the low [1PhEtOH] regime, analysis of the Eyring plot revealed a free energy activation barrier ($\Delta G^{\ddagger}$) of

DOI: 10.1021/acscatal.5b00952
ACS Catal. 2015, 5, 5468−5485

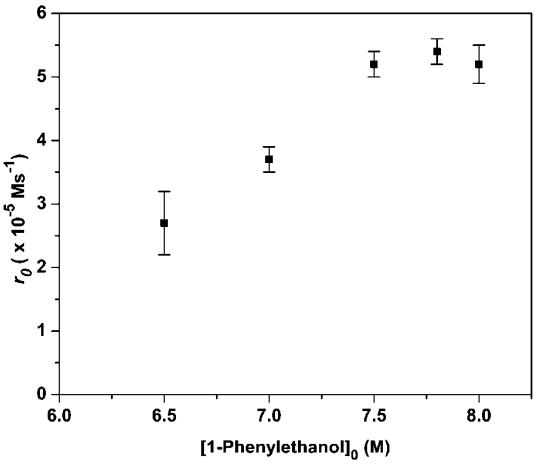

Figure 2. Influence of [1PhEtOH] on the reaction rates for 1PhEtOH dehydrogenation catalyzed by **3**.

31(3) kcal/mol at 120 °C, an activation enthalpy ($\Delta H^{\ddagger}$) of 18(1) kcal/mol, and an activation entropy ($\Delta S^{\ddagger}$) of −32(3) eu.[14] In the high [1PhEtOH] regime, analysis of the Eyring plot revealed a $\Delta G^{\ddagger}$ of 31(3) kcal/mol at 120 °C, an $\Delta H^{\ddagger}$ of 15(1) kcal/mol, and an $\Delta S^{\ddagger}$ of −41(3) eu. An activation enthalpy of this magnitude is consistent with bond-breaking character in the turnover-limiting transition structure.[15] In addition, the relatively large negative entropy of activation suggests not only an associative process but also a higher degree of organization in the transition state than in the ground state. Analysis of the activation parameters at low and high [1PhEtOH] revealed equivalent $\Delta G^{\ddagger}$ values. However, between the low and high [1PhEtOH] regimes, the magnitude of $\Delta H^{\ddagger}$ decreases, whereas that of $\Delta S^{\ddagger}$ increases. This implies that at high [1PhEtOH] the AAD catalysis is entropically controlled. Unfortunately, these Eyring data could not be used to unambiguously differentiate between the two proposed mechanisms. For example, a highly ordered transition structure could be expected for an alcohol-assisted proton/hydrogen-transfer turnover-limiting step in the two pathways as proposed in Scheme 5.[16] Furthermore, a range of $\Delta S^{\ddagger}$ values (+12 to −30 eu) have been reported for a β-H elimination turnover-limiting step from metal-alkoxide species.[17]

Isotopic Labeling Studies. A series of deuterium isotopic substitutions of 1PhEtOH were used to interrogate proton and hydride transfer and inner- versus outer-sphere pathways. The scenario of 1PhEtOH deprotonation as the turnover-limiting step was examined by monitoring the dehydrogenation of the 1PhEtOH isotopologue, 1PhEtOD, catalyzed by **3**. A normal primary kinetic isotope effect (KIE) would be anticipated if the O−H bond cleavage is involved in the turnover-liming step or precedes it. Dehydrogenation of 1PhEtOD at 120 °C in the presence of 0.01 mol % **3** yielded an observed rate of 2.7(1) × 10^{-5} M·s^{-1} (Scheme 6, eq 4). This reduced reaction rate, compared to the rate for the perprotio isotopologue, afforded a KIE (r_{OHCH}/r_{ODCH}) of 1.9(2), thus supporting either O−H bond cleavage in the turnover-limiting step (inner- or outer-sphere) or a β-H elimination turnover-limiting step with a proton-transfer pre-equilibrium (inner-sphere). Hence, it should be noted that the observed isotope effect is likely a composite of both equilibrium and kinetic isotope effects.[18]

Another set of isotopic labeling experiments were performed with a second isotopologue of 1PhEtOH, 1PhCH$_3$CDOH. An observed reaction rate of 3.6(1) × 10^{-5} M·s^{-1} was obtained for the dehydrogenation of 1PhCH$_3$CDOH at 120 °C resulting in a KIE (r_{OHCH}/r_{OHCD}) of 1.4(1) (Scheme 6, eq 5). This observed KIE is consistent with the cleavage of the C−H bond in the turnover-limiting step (β-H elimination or outer-sphere pathway) and is too large for a secondary isotope effect. Depending on the nature of the transition state, varying magnitudes of KIE (>1.3) have been measured for β-H elimination from metal-alkoxides.[18c] However, a KIE with a larger magnitude (2.6) was observed for an outer-sphere concerted pathway.[19] In addition, the measured KIE is also consistent with a proton-transfer turnover-limiting step where a Ru−H(D) species could participate in deprotonation of the alcohol after the first turnover in an inner-sphere pathway.

The outer-sphere concerted pathway can be evaluated using a series of isotopic labeling experiments. For example, Bäckvall and Johnson demonstrated that Shvo's catalyst operated via an outer-sphere concerted mechanism by analyzing the KIE for the doubly deuterium labeled isotopologue of 1PhEtOH, 1PhCH$_3$CDOD.[19] For a concerted pathway, the observed isotope effect for 1PhCH$_3$CDOD should be the product of the two individual isotope effects (r_{OHCH}/r_{ODCH} × r_{OHCH}/r_{OHCD}). When 1PhCH$_3$CDOD was subjected to the standard

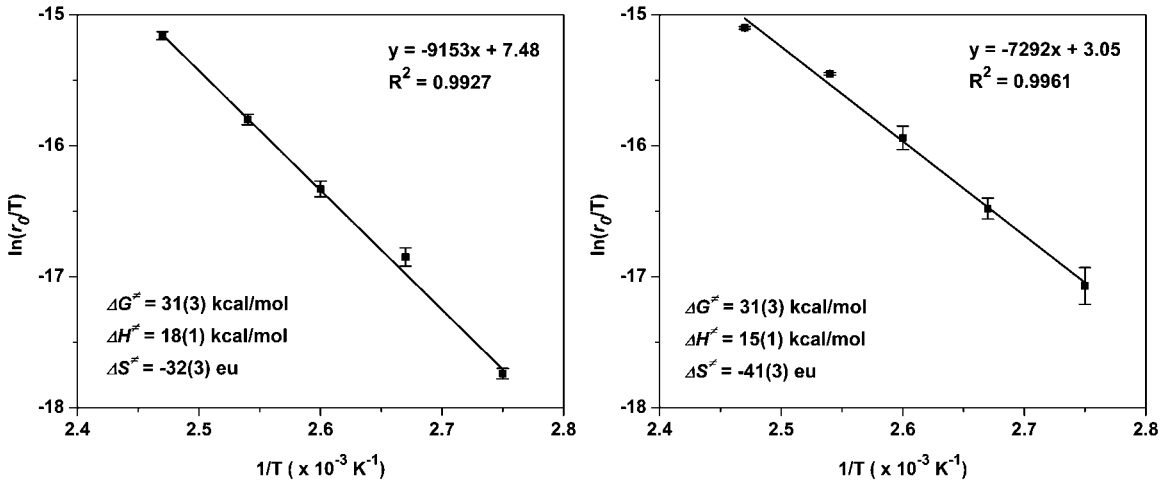

Figure 3. Eyring plots for 1PhEtOH dehydrogenation catalyzed by **3**. Left panel: [1PhEtOH]$_0$ = 7.5 M. Right panel: [1PhEtOH]$_0$ = 8.2 M.

DOI: 10.1021/acscatal.5b00952
ACS Catal. 2015, 5, 5468−5485

Scheme 5. Proposed 1PhEtOH Deprotonation with 1PhEtOH as a Proton-Transfer Shuttle in the Inner- and Outer-Sphere Pathways

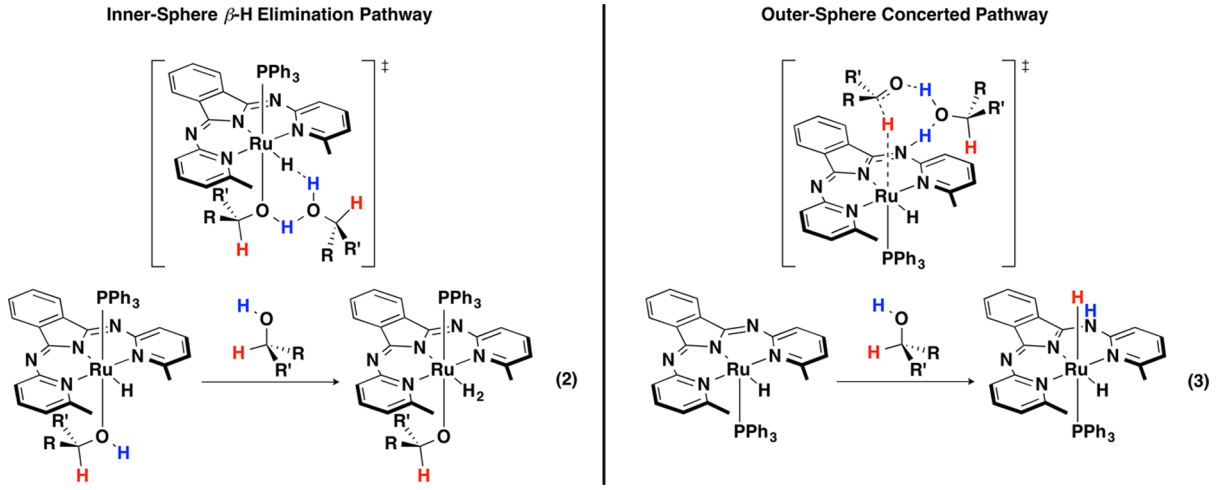

Scheme 6. Isotopic Labeling Experiments for the Dehydrogenation of 1PhEtOH

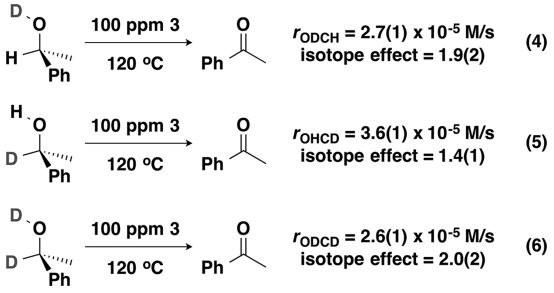

dehydrogenation conditions, a reaction rate of $2.6(1) \times 10^{-5}$ $M \cdot s^{-1}$ was observed, providing a kinetic isotope effect (r_{OHCH}/r_{ODCD}) of 2.0(2) (Scheme 6, eq 6). In contrast, the product of the individual isotope effects is 2.7 (1.9 × 1.4) and thus inconsistent with the measured combined KIE. Furthermore, to normalize for any secondary isotope effects on the C−H KIE, we averaged the r_{OHCH}/r_{OHCD} (1.44) and r_{ODCH}/r_{ODCD}(1.04) values to provide a C−H KIE of 1.24. The product of the O−H and averaged C−H KIE is 2.4(1), which also does not match the observed r_{OHCH}/r_{ODCD}. These analyses provide strong evidence *against* pathways in which both proton and hydride transfer in a concerted manner and are in support of an inner-sphere, stepwise pathway.

Synthesis and Reactivity of Ru(bMepi^{Me})(PPh$_3$)OTf$_2$: Possible Role of Metal−Ligand Cooperativity. To complement the kinetic isotope studies that discounted an outer-sphere concerted pathway, we targeted Ru^{II} compounds with the ligand bMepi^{Me}, in which one of the imine groups is methylated. Prior studies from our laboratory found that a late stage modification can be used to alkylate the imine backbone, thus providing complementary complexes that feature similar primary coordination environments yet differ in charge of the pincer ligand.[20] Furthermore, the site of protonation or alkylation in these and related complexes[21] is the imine nitrogen, rather than the amido nitrogen, which indicates the former as the favored kinetic site for protonation. Hence, metal−ligand cooperative pathways involving proton transfer to the central isoindoline nitrogen are unlikely AAD mechanisms for the bis(pyridylimino)isoindolate framework.

Ru(bMepi^{Me})(PPh$_3$)OTf$_2$ (**5**) was prepared by treating a DCM solution of Ru(bMepi)(PPh$_3$)Cl (**4**) with 10 equiv of MeOTf at room temperature for 18 h. Complex **5** was isolated in 62% yield and characterized by ^{1}H and ^{31}P NMR spectroscopy, elemental analysis, and X-ray crystallography. The ^{31}P{^{1}H} spectrum displays a singlet at 47.8 ppm, and the ^{1}H NMR spectrum is consistent with the asymmetry of the bMepi^{Me} ligand. In particular, two distinct resonances for the *ortho*-CH$_3$ groups were located at 1.57 and 1.78 ppm and a singlet was detected at 3.71 ppm and assigned as the methyl group on the ligand backbone. Complex **5** has a slightly distorted square-based pyramid (τ = 0.10)[22] structure, which contains a triflate anion *trans* to the PPh$_3$ ligand (Figure 4).

In addition to the covalent methylated imine bond in **5**, noncovalent interactions of the *ortho*-methyl groups were found. Agostic M−H−C interactions are characterized by

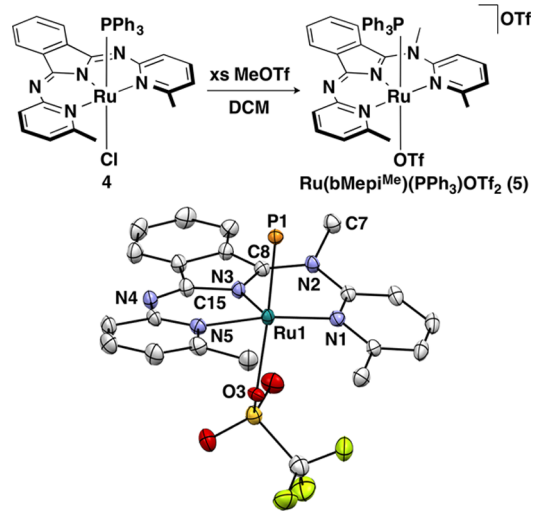

Figure 4. Synthesis and crystal structure (thermal ellipsoids of **5** depicted at 50% probability) of Ru(bMepi^{Me})(PPh$_3$)OTf$_2$ (**5**). The outer-sphere triflate anion, PPh$_3$ phenyl groups, and hydrogen atoms are omitted for clarity. Selected bond distances (angstroms): Ru1−P1, 2.2933(7); Ru1−N1, 2.081(3); Ru1−N3, 1.955(2); Ru1−N5, 2.063(3); Ru1−O3, 2.221(2); N2−C7, 1.488(4); N2−C8, 1.351(4); N3−C8, 1.340(4); N3−C15, 1.410(4); and N4−C15, 1.289(4).

DOI: 10.1021/acscatal.5b00952
ACS Catal. 2015, 5, 5468−5485

relatively short M−H distances (1.8 to 2.3 Å), small M−H−C bond angles (90 to 140°), and upfield chemical shifts of the agostic hydrogen atoms.[23] All three criteria for an agostic interaction are met in complex **5**. The crystal structure of **5** reveals a short M−H distance of 2.29 Å[24] and a small M−H−C bond angle of 119° from one hydrogen of the *ortho*-CH_3 groups. In addition, the two singlet resonances for the methyl groups are upfield of the free HbMepi ligand (the hydrogen atoms of the methyl groups on the free HbMepi ligand were observed in the ^{1}H NMR spectrum as a singlet at 2.50 ppm, Δ = 0.93, 0.72 ppm). The analogous protonated complex (Ru(HbMepi)(PPh_3)Cl[PF_6]) was also synthesized by heating a THF solution containing HbMepi, $RuCl_2(PPh_3)_3$, and $TlPF_6$ (Figure 5). In contrast to sharp ligand resonances observed in

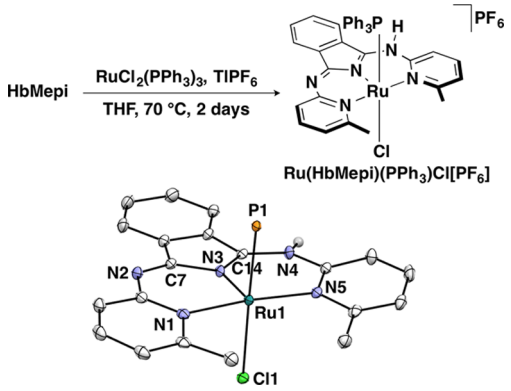

Figure 5. Synthesis and crystal structure (thermal ellipsoids of **5** depicted at 50% probability) of Ru(HbMepi)(PPh_3)Cl[PF_6]. The outer-sphere PF_6 anion, PPh_3 phenyl groups, and hydrogen atoms, except the NH, are omitted for clarity. Selected bond distances (angstroms): Ru1−P1, 2.3356(4); Ru1−N1, 2.048(1); Ru1−N3, 1.948(1); Ru1−N5, 2.100(3); Ru1−Cl1, 2.4696(3); N2−C7, 1.283(2); N3−C7, 1.412(2); N3−C14, 1.329(2); and N4−C14 1.339(2).

the ^{1}H NMR spectrum of **5**, the analogous protonated complex, Ru(HbMepi)(PPh_3)Cl[PF_6], contains broad ligand resonances at room temperature, which are consistent with a dynamic protonation equilibrium between the imine nitrogens. The solid-state structure shows square-based pyramid geometry about the Ru center with a chloride ligand *trans* to PPh_3. For Ru(HbMepi)(PPh_3)Cl[PF_6], two out of the three criteria are met for an agostic interaction; the M−H distance is slightly longer (2.44 Å). However, the M−H−C bond angle of 107° and the upfield shift of the *ortho*-CH_3 groups (1.78 and 1.70 ppm; Δ = 0.72, 0.80 ppm) are consistent with an agostic M−H−C interaction. Complex **4** exhibited similar structural and spectroscopic properties as the protonated complex, such as the M−H distance (2.41 Å), a M−H−C bond angle of 113°, and the upfield shift of the *ortho*-CH_3 groups (1.72 ppm; Δ = 0.78 ppm).

Because the isotopic labeling studies were not consistent with a concerted dehydrogenation pathway (vide supra), a stepwise, hybrid metal−ligand cooperative pathway was evaluated. This bifunctional hybrid mechanism is a combination of the inner-sphere β-H elimination and the outer-sphere bifunctional pathway, in which proton transfer takes place at the backbone imine group on the bMepi ligand, affording a Ru-alkoxide intermediate (Scheme 7, eq 7) that could undergo β-H elimination. Unless H_2 is eliminated, this pathway is not probable because the Ru-alkoxide intermediate is an 18 e$^-$

Scheme 7. Proposed Proton Transfer via Step-Wise Metal−Ligand Cooperativity

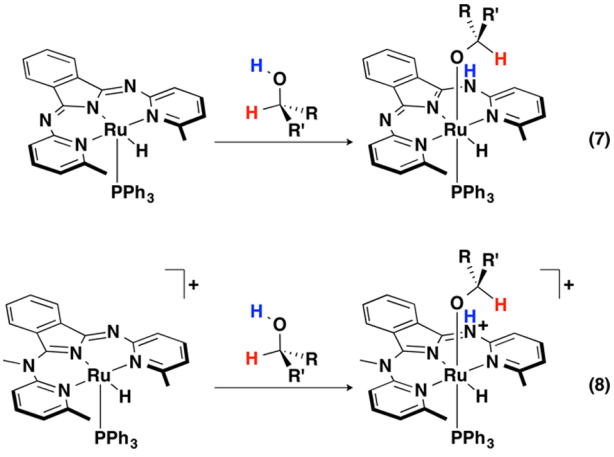

species and could not undergo β-H elimination without losing another ligand (or dissociation of the alkoxide or a pyridine arm). Dissociation of the PPh_3 ligand would deviate from the observed zero-order [PPh_3] dependence.

To assess the potential participation of the backbone imine group on the bMepi ligand in the dehydrogenation of alcohols via bifunctional metal−ligand catalysis, the dehydrogenation of 1PhEtOH catalyzed by **5** was evaluated. Of key importance to a bifunctional metal−ligand pathway is proton transfer to the backbone imine nitrogen. This protonation event would seem energetically unfavorable for the alkylated complex (Scheme 7, eq 8) given that heating **4** in excess MeOTf afforded only the monomethylated complex, which suggests that the remaining imine functionality is less basic in the bMepi^{Me} ligand than in the parent bMepi ligand.

The proposed hybrid metal−ligand cooperative pathway was evaluated by comparing the reaction rates of 1PhEtOH dehydrogenation catalyzed by **4** and **5** (Scheme 8). Heating a

Scheme 8. Reaction Rate Comparison between the bMepi and bMepi^{Me} Ligated Ruthenium Complexes

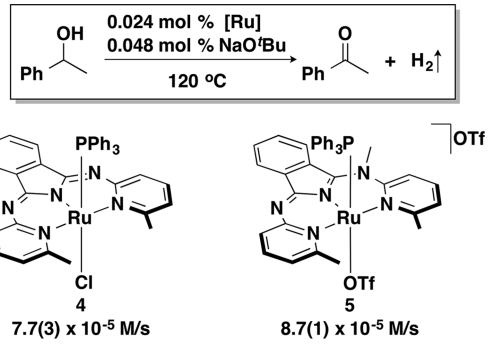

7.8 M 1PhEtOH solution containing 0.024 mol % of **4** and 0.048 mol % NaO^{t}Bu to 120 °C for 4 h resulted in an averaged TON of 1441, which corresponds to a reaction rate of 7.7(3) × 10^{-5} M·s^{-1}. The alkylated Ru complex (**5**) was also a competent dehydrogenation precatalyst. For instance, under the same reaction conditions, complex **5** oxidized 1PhEtOH to acetophenone and H_2 with a reaction rate of 8.7(1) × 10^{-5} M·s^{-1}.[25] These results demonstrate that a cooperative interaction involving the imine functionality is not necessary to achieve efficient rates for catalytic AAD reaction.[26]

DOI: 10.1021/acscatal.5b00952
ACS Catal. 2015, 5, 5468−5485

Hammett Studies. The electronic character of the turnover-limiting transition state in catalytic AAD promoted by **3** was investigated by conducting a linear free energy analysis using initial rates of dehydrogenation of *para*-substituted 1PhEtOH substrates (Figure 6). The ρ value has previously

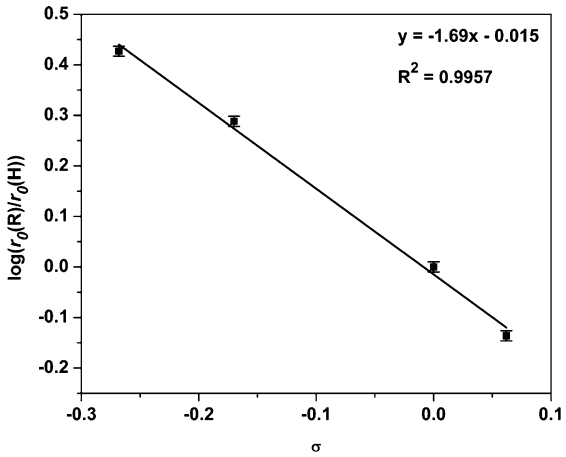

Figure 6. Hammett plot for 1PhEtOH dehydrogenation catalyzed by **3**.

been used to differentiate between limiting mechanistic regimes of alcohol dehydrogenation (Scheme 9). For instance, distinct

Scheme 9. Comparison of Hammett Parameters

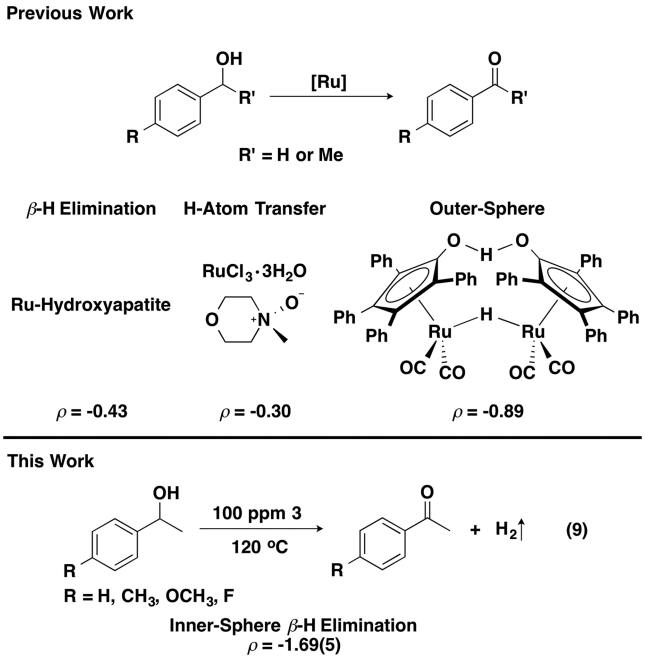

ρ values were reported for Ru-catalyzed alcohol dehydrogenation reactions that operate through turnover-limiting β-H elimination (ρ = −0.43),[27] free-radical H atom transfer (ρ = −0.30),[28] or outer-sphere pathway (ρ = −0.89).[29] In contrast to these values, the Hammett analysis for **3** afforded a ρ value of −1.69(5). The negative ρ value signifies a positive charge buildup in the transition state, supporting a β-H elimination turnover-limiting step in the inner-sphere pathway. Although **3** and the heterogeneous Ru-hydroxyapatite system are proposed to undergo a β-H elimination turnover-limiting step, the difference in magnitude of the ρ values may be explained by the nature of the transition state. The smaller ρ value of −0.43 observed for Ru-hydroxyapatite indicates that electronic changes have a subtle effect on β-H elimination, which is consistent with a late transition state with almost complete C−H bond cleavage and Ru−H bond formation. For our system **3**, electron-donating groups increase the nucleophilicity of the benzylic hydrogen atom, which acquires hydridic character during β-H elimination. Stabilization of the positive charge buildup at the benzylic carbon as the hydride is transferred in the transition state suggests an early transition-state model.

Isolation of a Ruthenium(II)−Alkoxide Complex. Following the kinetic experiments, which support an inner-sphere β-H elimination pathway, stoichiometric reactions were performed to examine the intermediate species during catalysis. In particular, a Ru alkoxide species was implicated as the catalyst resting state that undergoes β-H elimination in an inner-sphere pathway. To trap such a species prior to β-H elimination, trifluoroethanol, whose conjugate base is resistant to β-H elimination,[30] was selected. The addition of 1.1 equiv of trifluoroethanol to a solution of **3** in THF resulted in the clean conversion to Ru(bMepi)(PPh_3)(OCH_2CF_3) (**6**), which was isolated as a dark blue solid in 76% yield after heating at 70 °C for 2 days (Figure 7). The ^{1}H NMR spectrum features a single

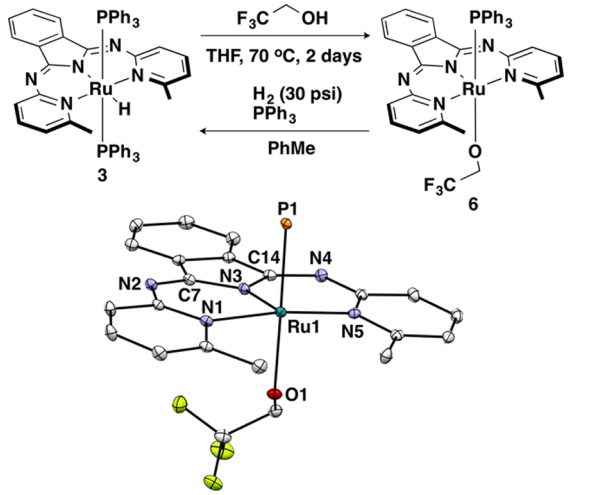

Figure 7. Synthesis and crystal structure (thermal ellipsoids of **6** depicted at 50% probability) of Ru(bMepi)(PPh_3)(OCH_2CF_3) (**6**). PPh_3 phenyl groups and hydrogen atoms are omitted for clarity. Selected bond distances (angstroms): Ru1−P1, 2.3224(5); Ru1−O1, 2.086(1); Ru1−N1, 2.079(2); Ru1−N3, 1.946(2); Ru1−N5, 2.075(2); N2−C7, 1.298(3); N3−C7, 1.380(3); N3−C14, 1.374(3); and N4−C14, 1.304(3).

set of bMepi resonances with the methyl resonances at 1.75 ppm, and the ^{31}P{^{1}H} NMR spectrum of **6** exhibits a singlet at 43.8 ppm, which is similar to the ^{31}P spectrum observed for Ru(bMepi)(PPh_3)Cl (**4**, 43.5 ppm). Crystals suitable for single-crystal X-ray diffraction were obtained from vapor diffusion of pentane into a PhMe solution of **6**. The solid-state structure shows a square-based pyramid geometry about the Ru^{II} center (τ = 0.01)[22] with the $-OCH_2CF_3$ ligand *trans* to PPh_3 (Figure 7). The shortest M−H distance is 2.69 Å with a M−H−C bond angle of 99°, and the chemical shift of the methyl groups is upfield of the free HbMpi ligand. The structural and spectroscopic properties satisfy two out of three criteria for

DOI: 10.1021/acscatal.5b00952
ACS Catal. 2015, 5, 5468−5485

determining an agostic interaction between the Ru center and the methyl C−H group.

Given that complex **6** is similar to the proposed Ru-alkoxide intermediate in the AAD catalytic cyclc, intermediates species prior to H_2 liberation were investigated by allowing **6** to react with H_2. When a J. Young NMR tube containing a toluene-d_8 solution of **6** and PPh_3 was charged with 30 psi of H_2, the immediate formation of trifluoroethanol was detected as a triplet at −76.5 ppm in the proton-coupled ^{19}F spectrum, and **6** and **3** were the *only* complexes observed by ^1H and ^{31}P NMR spectroscopy. In addition, no reaction was observed when the same experiment was performed at −75 °C. Upon slowly warming the J. Young tube in the NMR spectrometer, the formation of trifluoroethanol and **3** resulted from the clean conversion of **6** and H_2. No Ru intermediate species were observed at low temperature, and **3** was the only Ru species observed when **6** reacted with H_2. These observations suggest that both alcohol and η^2-H_2 adducts are short-lived intermediates with respect to the alkoxide and/or **3**. Furthermore, no reaction (β-H elimination or decomposition) was observed when a solution of **6** with and without 100 equiv of trifluoroethanol in C_6D_6 was heated to operating temperatures for catalytic AAD reaction (120 °C for 3 h), which is consistent with an increase (∼15 kcal/mol) in the activation barrier effected by the trifluoromethyl group.[30a]

Catalyst Resting State and Mechanistic Discussion. With known spectroscopic features of a Ru-bMepi alkoxide species in hand, NMR experiments were performed to observe the catalyst resting state in situ. A solution of 8.3 M 1PhEtOH containing 0.1 mol % of **3** inside a J. Young tube was monitored by ^1H and ^{31}P NMR spectroscopy at ambient temperature and 100 °C. After 10 min at ambient temperature, 73% of **3** was converted to a new species with a ^{31}P resonance at 41.7 ppm with concomitant formation of free PPh_3. The hydride region of the ^1H NMR spectrum showed no new species. This new species at 41.7 ppm is consistent with the chemical shift of the isolated Ru alkoxide **6** and thus is proposed as Ru(bMepi)-(PPh_3)(OCHPhMe).[31] Heating the J. Young tube inside the NMR spectrometer for 10 min at 100 °C resulted in the full conversion of **3** to the proposed Ru alkoxide. At 100 °C the ^{31}P NMR spectrum exhibited only two resonances corresponding to the Ru alkoxide (40.6 ppm) and free PPh_3 with 1:1 integration values. Observation of the catalyst resting state as Ru-alkoxide species at high [1PhEtOH] further supports a β-H elimination turnover-limiting step during catalysis.

The catalyst resting state was also examined at low [1PhEtOH]. A C_6D_6 solution containing 0.83 M 1PhEtOH and 0.1 mol % of **3** was monitored by ^1H and ^{31}P NMR spectroscopy at ambient temperature and 100 °C. After 10 min at ambient temperature, 13% of a species consistent with formulation of the proposed alkoxide (^{31}P = 41.7 ppm) was observed by ^{31}P NMR spectroscopy. The hydride region of the ^1H NMR spectrum showed only the hydride resonance of **3** as a triplet, which was broadened and suggestive of a dynamic process associated with ligand substitution and/or proton transfer. The equilibrium constant between **3** and the proposed Ru-alkoxide species is invariant from 0.83 to 6.0 M 1PhEtOH, which is consistent with a pre-equilibrium process (Table S1). After the NMR tube was heated for 10 min at 100 °C, a 1:1 ratio of the Ru alkoxide to **3** was observed. Continued monitoring of the reaction mixture at 100 °C for 1 h (corresponding to ca. 0.3% acetophenone) resulted in no change in the ratio of the alkoxide species to **3**. This suggests that at low alcohol concentrations proton transfer is much slower and becomes competitive with β-H elimination. Thus, as reactant alcohol is consumed during catalysis, the turnover-limiting step is proposed to change from β-H elimination to proton transfer.

With the results of catalyst resting state at low and high [1PhEtOH] in hand, an in-depth analysis of [PPh_3] dependence, [1PhEtOH] dependence, and activation parameters was pursued. The reaction rate dependence on [1PhEtOH] fits a pre-equilibrium model with an equilibrium proton-transfer step occurring before turnover-limiting β-H elimination. This is consistent with the zero-order dependence on [PPh_3] and our previous analysis showing that phosphine binding is not in an equilibrium with the turnover-limiting step. At high [1PhEtOH], the forward rate of proton transfer is fast and β-H elimination is the turnover-limiting step. As [1PhEtOH] decreases, proton transfer becomes slower and eventually becomes turnover-limiting. This implies that the Eyring data collected at low [1PhEtOH] contains contributions from both proton transfer and β-H elimination with β-H elimination as the major component. Hence, the activation parameters ($\Delta H^{\ddagger}$ = 15 kcal/mol and $\Delta S^{\ddagger}$ = −41 eu) determined at high [1PhEtOH] exclusively describe the transition-state structure for a β-H elimination turnover-limiting step.

Although experimental evidence supports a β-H elimination turnover-limiting step, the large negative $\Delta S^{\ddagger}$ differs significantly from the previously reported values for β-H elimination from metal-alkoxide species.[17] The classic β-H elimination process involves cleavage of a β-C−H of the coordinated alkoxide, with concomitant formation of hydride on an empty *cis* coordination site and coordinated ketone (or aldehyde) ligand. It follows that β-H elimination reactions are typically unimolecular and largely enthalpically controlled (considerable bond making and breaking character in the transition state). To account for the atypical activation parameters for **3**, alternative mechanisms, such as binuclear hydride abstraction[32] and alcohol-assisted alkoxide dissociation,[33] for β-H elimination were considered. Our kinetic experiments discredit both processes as possible β-H elimination pathways for our catalyst. A binuclear mechanism is inconsistent with the observed first-order dependence on [**3**]. An alcohol-assisted alkoxide dissociative pathway is also unlikely because of the zero-order dependence on [1PhEtOH] at high [1PhEtOH]. Alternatively, we propose that **3** operates under a traditional β-H elimination process in which the highly negative activation entropy reflects contributions from solvent reorganization likely imparted by hydrogen bonding.[34] Such large entropic contributions are consistent with the reactions performed in neat alcohol solvent that allows the formation of a network of hydrogen bonds with a coordinated alkoxide ligand. Comparison of the activation parameters at low and high [1PhEtOH] revealed that entropy, not enthalpy, is the main contributor to the β-H elimination process. Thus, reorganization in the transition state, as reflected by the negative and large $\Delta S^{\ddagger}$, must be due to rearrangement of the hydrogen bonds interacting with the Ru-alkoxide species in order for the β-C−H to migrate onto the Ru center.

Proposed Mechanism. Based on the series of kinetic and isotopic labeling experiments, an inner-sphere catalytic cycle for 1PhEtOH dehydrogenation mediated by **3** is implicated. We propose that a single PPh_3 dissociation from **3** generates a coordinatively unsaturated Ru^{II}-hydride species that can reversibly bind 1PhEtOH. This species likely undergoes a fast proton-transfer event in equilibrium with a β-H elimination

DOI: 10.1021/acscatal.5b00952
ACS Catal. 2015, 5, 5468−5485

turnover-limiting step to yield the ketone product and generate the coordinatively unsaturated Ru^{II}-hydride species to re-enter in the dehydrogenation cycle (Scheme 10).

Scheme 10. Proposed Mechanism for AAD Catalyzed by 3

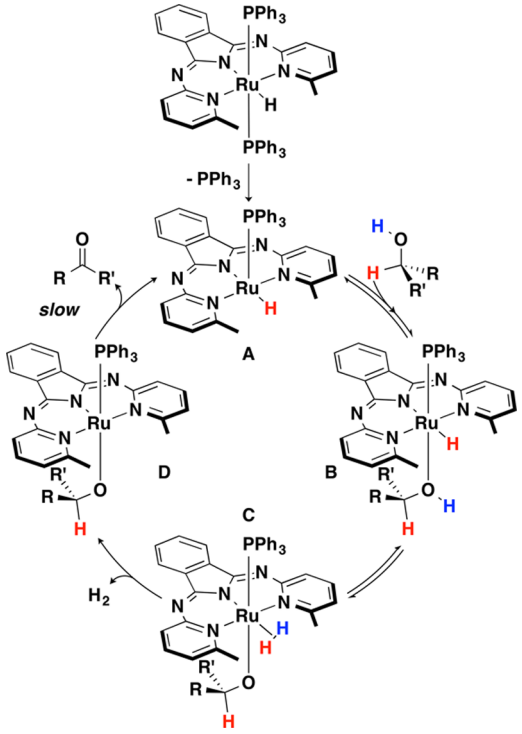

Primary versus Secondary Alcohol Dehydrogenation. An unusual feature of precatalyst **3** is the high selectivity for secondary alcohol dehydrogenation in the presence of primary alcohols.[35] To a first approximation, thermodynamic arguments might be invoked to support the formation of the ketone over the aldehyde product.[36] However, this consideration assumes equilibrium conditions are met, which is not likely under the catalytic conditions. To gain further insight into the origin of the chemoselectivity bias, we evaluated competition experiments between benzyl alcohol (BnOH) and 1PhEtOH. Heating an equimolar (0.5 mmol) mixture of BnOH and 1PhEtOH containing 5 mol % **3** to 100 °C for 3 h resulted in the quantitative conversion of 1PhEtOH to acetophenone, while BnOH remained unreacted (Scheme 11, eq 10). This result is consistent with our previously reported findings that dehydrogenation of secondary alcohols is favored in the presence of primary alcohols when using temperatures lower than those required for acceptorless dehydrogenative coupling reactivity to afford esters.[8] However, because these conditions do not afford coupling reactivity of primary alcohols, more forcing conditions were used to promote dehydrogenation activity of primary and secondary alcohols. Heating a PhMe solution containing BnOH and **3** (5 mol %) to 120 °C for 3 h afforded 65% benzyl benzoate and 5% benzaldehyde (Scheme 11, eq 12).

Scheme 11. Competition Experiment between BnOH and 1PhEtOH[a]

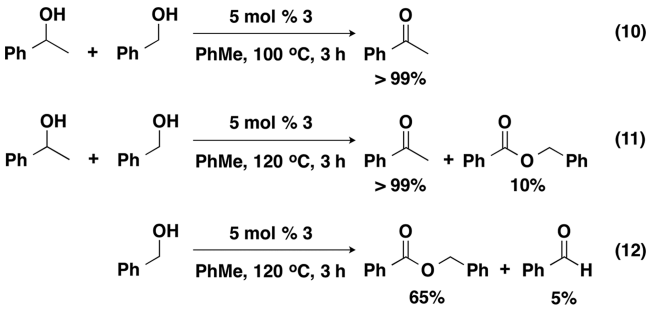

[a]Note that reaction yields are calculated based on the corresponding alcohol reactants.

When a competition experiment using BnOH and 1PhEtOH was performed under identical reaction conditions, 10% benzyl benzoate and >99% acetophenone were observed (Scheme 11, eq 11). These results demonstrate that **3** chemoselectively dehydrogenates secondary alcohols in the presence of primary alcohols under conditions which promote the dehydrogenation of both primary and secondary alcohols. The origin of this preference was considered to arise from differences in rates of either (a) proton transfer or (b) β-H elimination. In addition to implications of β-H elimination, rather than proton transfer, as the turnover-limiting step, the pK_a difference between primary (pK_a(*n*-PrOH) = 16.0) and secondary (pK_a(^{i}PrOH) = 16.5) alcohols also cannot account for the observed chemoselectivity because primary alcohols are more acidic and should be easily deprotonated.[37] To further support this hypothesis, in situ examination of the catalyst resting state by ^{31}P NMR spectroscopy revealed the quantitative formation of a primary Ru-alkoxide species (^{31}P = 42.5 ppm) when 0.2 mol % of **3** was dissolved in a 4.3 M BnOH C_6D_6 solution at room temperature. In a different experiment under identical conditions using 4.3 M 1PhEtOH, only 45% of **3** was converted to the secondary Ru-alkoxide species as observed in the ^{31}P NMR spectrum. Thus, the origin of the observed chemoselectivity must occur *after* the formation of the Ru-alkoxide intermediate.

To address chemoselectivity-inducing β-H elimination-dependent reactions, we monitored the catalyst resting state and product(s) formation of an AAD reaction of a 1:1 mixture of BnOH (4.3 M) to 1PhEtOH (4.3 M) catalyzed by 0.2 mol % of **3**. Prior to heating the reaction to 120 °C, the ^{31}P NMR spectrum exhibited only two resonances: one for free PPh_3 and another at 42.5 ppm, which was previously identified as the primary Ru-alkoxide species (Ru(bMepi)(PPh_3)(OCH_2Ph). Upon heating the reaction to 120 °C, a 9:1 ratio of the primary to secondary alkoxide species were observed. Continuous monitoring of the reaction showed no changes in the ratio of the primary to secondary alkoxides species in the ^{31}P NMR spectrum and *only* the production of acetophenone (34 turnovers in 30 min) was observed in the ^{1}H NMR spectrum (Scheme 12).

The competition experiments implicate slower β-H elimination from the primary alkoxide compared to the secondary alkoxide, which is consistent with the absence of BnOH dehydrogenation activity at lower (<120 °C) temperatures, and the stronger BDE of the C−H bond cleaved.[38] In addition, the activation parameters at high alcohol concentration for β-H elimination suggests that hydride transfer is dominated by entropic factors derived from hydrogen-bonding solvation effects. Hydrogen bonding with the alcohol solvent would be more favorable for the primary alkoxide species because of the decreased steric environment surrounding the oxygen atom (−$OCPhH_2$ versus −OCPhMeH). Therefore, a higher degree

DOI: 10.1021/acscatal.5b00952
ACS Catal. 2015, 5, 5468−5485

Scheme 12. Catalyst Resting State and Activity for a Competitive Experiment between BnOH and 1PhEtOH

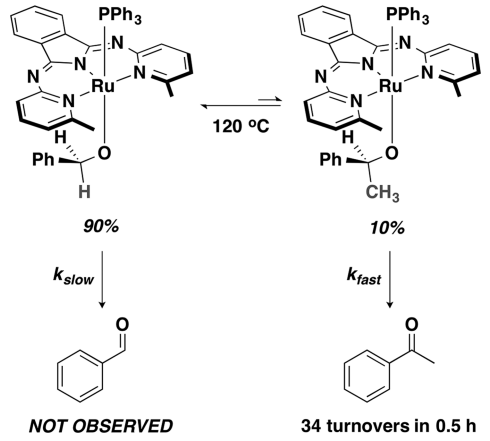

of reorganization in the transition state for β-H elimination would be anticipated for the primary alkoxide species, thus leading to a larger kinetic barrier.

Steric and Electronic Effects of the bMepi Ligand on Dehydrogenation Activity. The requirement of the *ortho*-methyl units around the primary coordination sphere was interrogated with the ligands 1,3-bis(4′,6′-methyl-2′-pyridylimino)isoindolate (b4,6-Mepi) and 1,3-bis(2′-pyridylimino)isoindolate (bpi). Complementary to evaluation of a steric effect, the effects of electronically rich and deficient ligands were also examined using para-substituted variants, b4Rpi (R = H, Cl, Me, OMe, OH). A series of Ru(b4Rpi)-$(PPh_3)_2Cl$ (**7-R**, R = H, Cl, Me, OMe) complexes were synthesized by heating a THF solution containing Hb4Rpi, $RuCl_2(PPh_3)_3$, and $TlPF_6$ to 60−70 °C for 16−24 h, followed by the addition of 1.05 equiv of NaO^{t}Bu (Figure 8). After isolation of complexes **7-R**, the composition and purity were confirmed by ^{1}H, ^{13}C, and ^{31}P NMR spectroscopy, infrared spectroscopy, and elemental analysis. The ^{1}H NMR spectra of **7-R** feature a single set of ligand-based resonances with the absence of the isoindole proton, and the $^{31}P\{^1H\}$ NMR spectra exhibit a singlet at 26.1, 25.1, 26.1, and 26.4 ppm (**7-R**, R = H, Cl, Me, OMe, respectively), consistent with *trans* disposed phosphorus atoms and meridional binding of the b4Rpi ligand. Single crystals of **7-H** and **7-CH$_3$** were subjected to X-ray diffraction experiments, and the solid-state structures confirm octahedral geometry around the Ru^{II} center with a chloride ligands *trans* to the isoindolate nitrogen atom (Figure 8).

To enhance the stability of a coordinatively unsaturated Ru species during AAD catalysis, we targeted an electron-rich metal environment by synthesizing a Ru compound with the ligand b4OHpi, in which strongly electron-donating hydroxyl groups are substituted *para* to the pyridyl nitrogens. Deprotonation of the hydroxyl groups to generate aryl-oxide groups in situ would further enhance the electron-richness of the metal environment. Ru(b4OHpi)$(PPh_3)_2Cl$ (**7-OH**) was prepared by allowing a THF solution containing Hb4OHpi, $RuCl_2(PPh_3)_3$, and NaO^{t}Bu to stir at 70 °C for 16 h. **7-OH** was isolated in 79% yield as a dark blue solid with only slight solubility in THF. The ^{1}H NMR spectrum reveals multiple broad resonances, and the $^{31}P\{^1H\}$ NMR spectrum in THF displays resonances at 68.38, 26.19, and −5.51 ppm (free PPh_3), suggesting a dynamic process likely caused by the dissociation of one of the PPh_3 ligands in solution. This

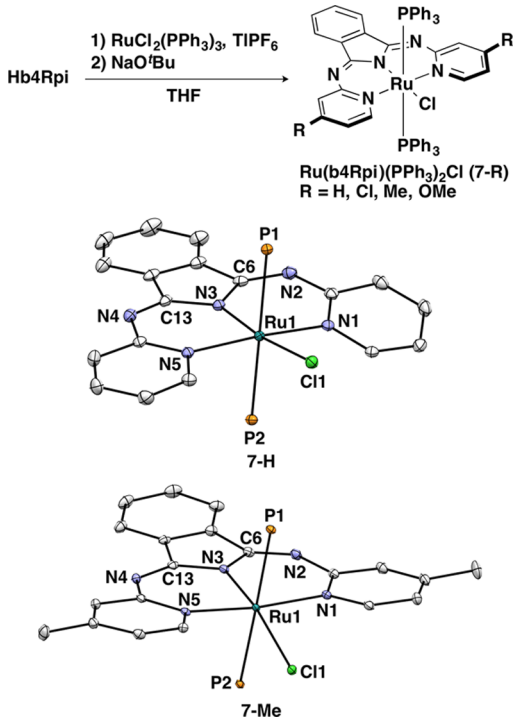

Figure 8. Synthesis of Ru(b4Rpi)$(PPh_3)_2Cl$ (**7-R**) and crystal structures (thermal ellipsoids depicted at 50% probability) of **7-H** and **7-Me**. The PPh_3 phenyl groups and hydrogen atoms are omitted for clarity. Selected bond distances for **7-H** (angstroms): Ru1−Cl1, 2.4782(4); Ru1−P1, 2.4275(4); Ru1−P2, 2.3874(4); Ru1−N1, 2.092(1); Ru1−N3, 2.009(1); Ru1−N5, 2.116(1); N2−C6, 1.302(2); N3−C6, 1.367(2); N3−C13, 1.371(2); and N4−C13, 1.299(2). Selected bond distances for **7-Me** (angstroms): Ru1−Cl1, 2.4824(5); Ru1−P1, 2.4076(5); Ru1−P2, 2.4254(5); Ru1−N1, 2.111(2); Ru1−N3, 2.004(2); Ru1−N5, 2.101(2); N2−C6, 1.304(3); N3−C6, 1.365(3); N3−C13, 1.379(3); and N4−C13, 1.296(3).

solution dissociation dynamics was suppressed with the addition of excess PPh_3. For example, in the presence of 1 equiv of PPh_3, the singlet at 68.38 ppm was absent in the $^{31}P\{^1H\}$ NMR spectrum. Crystals suitable for single-crystal X-ray diffraction were obtained from vapor diffusion of pentane into a THF solution of **7-OH** at −35 °C. Analogous to the single-crystal structures for **7-H** and **7-Me**, the solid-structure reveals an octahedral geometry around the Ru^{II} center with the b4OHpi ligand meridionally coordinated with two *trans* PPh_3 ligands and a chloride, thus confirming the identity of the product (Figure 9).

In the proposed AAD mechanism shown in Scheme 10, the steric profile of the methyl groups may play a blocking role to impede hydride transfer in the turnover-limiting step. This steric effect imposed by the methyl groups was examined by comparing the reaction rates of 1PhEtOH dehydrogenation catalyzed by **4**, **4-Me** (Ru(b4,6-Mepi)$(PPh_3)Cl$), **7-H**, and **7-Me** (Table 1). The reaction rates for **4** ($7.7(3) \times 10^{-5}$ M·s^{-1}) and **4-Me** ($7.7(3) \times 10^{-5}$ M·s^{-1}) were identical (Table 1, entries 1 and 2), which suggests that the weakly electron-donating methyl groups have no electronic effect on the dehydrogenation activity. This observation allowed evaluation of the steric influence of the *ortho*-methyl substituents of the bMepi ligand by comparing the reaction rates of **4** and **7-H**. The reaction rate was increased by 42% when **7-H** ($10.9(2) \times 10^{-5}$ M·s^{-1}, Table 1, entry 3) or **7-Me** ($10.9(2) \times 10^{-5}$ M·s^{-1},

DOI: 10.1021/acscatal.5b00952
ACS Catal. 2015, 5, 5468−5485

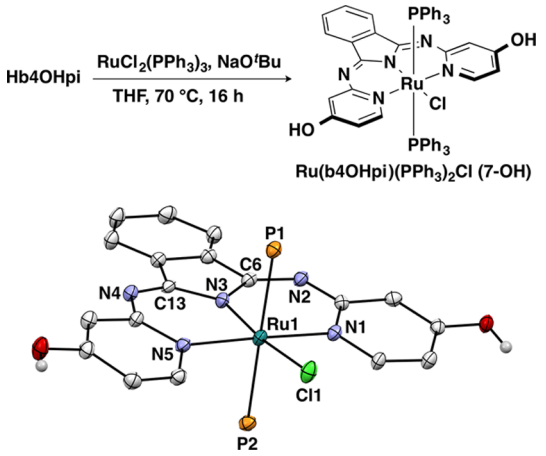

Figure 9. Synthesis and crystal structure (thermal ellipsoids depicted at 50% probability) of Ru(b4OHpi)$(PPh_3)_2$Cl (**7-OH**). The PPh_3 phenyl groups and hydrogen atoms are omitted for clarity. Selected bond distances (angstroms): Ru1−Cl1, 2.4824(5); Ru1−P1, 2.4076(5); Ru1−P2, 2.4254(5); Ru1−N1, 2.111(2); Ru1−N3, 2.004(2); Ru1−N5, 2.101(2); N2−C6, 1.304(3); N3−C6, 1.365(3); N3−C13, 1.379(3); and N4−C13, 1.296(3).

Table 1. Reaction Rates of 1PhEtOH Dehydrogenation[a]

entry	catalyst	rate ($\times 10^{-5}$ M·s^{-1})
1	**4**	7.7(3)
2	**4-Me**	7.7(3)
3	**7-H**	10.9(2)
4	**7-Me**	10.9(2)
5	**7-Cl**	8.0(5)
6	**7-OMe**	11.8(2)
7	**7-OH**	12.0(2)
8[b]	**7-OH**	13.3(2)
9[b]	**7-H**	12.4(2)

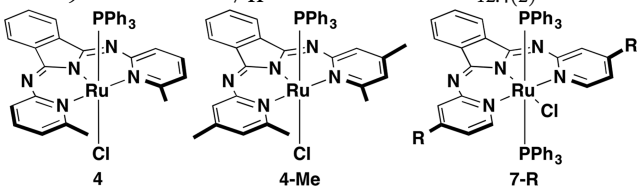

[a]Reaction conditions: 1PhEtOH (7.8 M), PhTMS (0.38 M), [Ru] (1.9 mM), and NaO^{t}Bu (3.8 mM) were stirred at 120 °C in an open vial inside an inert-atmosphere glovebox. The conversion of 1PhEtOH to acetophenone was monitored by ^{1}H NMR spectroscopy. [b]Reaction performed with 9.5 mM NaO^{t}Bu.

Table 1, entry 4) was used instead of **4**. The rate enhancement is consistent with a sterically blocking effect of the methyl groups, which hinders β-H elimination in the turnover-limiting step (Scheme 10).

While the addition of a modestly donating methyl group in the *para*-position had no effect on the overall rate, we evaluated the effect of adding highly donating substituents to the flanking pyridine rings. Increased electron donor strength of the ligand is expected to concomitantly enhance the hydricity of any metal-based hydrides.[39] However, because the turnover-limiting step is β-H elimination, the ligand electronic effect on the turnover-limiting step may be less than dramatic.

The electronic variations at the Ru center imposed by electronically rich and deficient bpi ligands were evaluated by examining the dehydrogenation rates of 1PhEtOH. The reaction rate was increased when **7-OMe** (11.8(2) $\times 10^{-5}$ M·s^{-1}; σ_{para}(OMe) = −0.27;[40] Table 1, entry 6) and **7-OH** (12.0(2) $\times 10^{-5}$ M·s^{-1}; σ_{para}(OH) = −0.37;[40] Table 1, entry 7) were used instead of **7-Cl** (8.0(5) $\times 10^{-5}$ M·s^{-1}; σ_{para}(Cl) = 0.23;[40] Table 1, entry 5). To further enhance the donor strength, the aryl-oxide (**7-O$^-$**; σ_{para}(O$^-$) = −0.81)[40] was prepared. **7-OH** was allowed to react with 5 equiv of NaO^{t}Bu, which resulted in a further 11% increase in rate (13.3(2) $\times 10^{-5}$ M·s^{-1}; Table 1, entry 8) of 1PhEtOH dehydrogenation. Although, these results indicate that a more electron-rich Ru environment exhibits higher AAD activity, the changes to the reaction rate are small; thus, the electronic environment at the Ru center has a minimal effect on the turnover-limiting step in the AAD catalytic cycle.

Base-Promoted AAD Catalysis. Benchtop-stable reagents provide greater synthetic utility and accessibility and thus are more commonly and easily handled by most synthetic laboratories. The air-sensitive precatalyst **3** is capable of mediating promoterless AAD reactions, likely due in part to the Ru-hydride, an internal basic site. Alternatively, entry into the AAD catalytic cycle should also be possible using the air-stable complex **4** in the presence of an external base or using an in situ preparation of the Ru-bMepi catalytic species. Indeed, when a toluene solution containing 0.5 mmol of 1PhEtOH, 1 mol % of **4**, and 2 mol % of NaO^{t}Bu was heated to reflux for 4 h, acetophenone was observed in quantitative (>99%) yield (Scheme 13, eq 13). This reactivity demonstrates the synthetic applicability of **4** as a dehydrogenation catalyst that can be prepared using air-stable reagents. Furthermore, AAD catalysis by in situ formation of the catalytically active Ru-bMepi species was evaluated. In the presence of 1 mol % $RuCl_2(PPh_3)_3$, 1 mol % HbMepi, and 3 mol % NaO^{t}Bu, 1PhEtOH was converted to acetophenone in >99% yield after heating for 4 h in refluxing toluene (Scheme 13, eq 14). Control experiments showed no reaction in the absence of HbMepi. Therefore, the broad applicability of our system to promote dehydrogenation by well-defined precatalysts as well as in situ generation from air-stable precursors highlights the robustness of the system.

Scheme 13. Base-Promoted AAD Catalysis

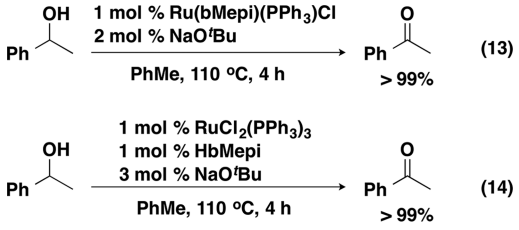

In addition to the alcohol dehydrogenation activity of the in situ prepared catalyst, stoichiometric reactions were performed to uncover intermediates en route to the well-defined precatalyst **4**. Allowing HbMepi and $RuCl_2(PPh_3)_3$ to react in dichloroethane at 70 °C for 4 h generated Ru(HbMepi)-$(PPh_3)_2Cl_2$ (**8**) in 70% yield as a green solid (Figure 10). The ^{31}P{^{1}H} spectrum displays a singlet at 24.9 ppm, and the ^{1}H NMR spectrum reveals a solution structure consistent with asymmetric binding of the HbMepi ligand. For example, two resonances for the *ortho*-CH_3 substituents were observed at 0.99 and 2.31 ppm, and nine distinct resonances were observed for the HbMepi scaffold in the aromatic region of the ^{1}H NMR spectrum. Crystals suitable for a single X-ray diffraction

DOI: 10.1021/acscatal.5b00952
ACS Catal. 2015, 5, 5468−5485

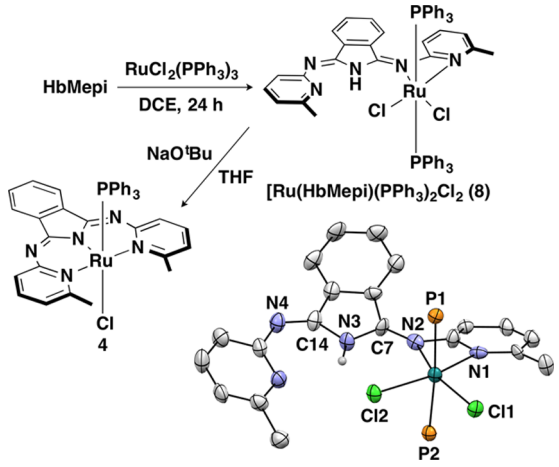

Figure 10. Synthesis of Ru(HbMepi)$(PPh_3)_2Cl_2$ (**8**) and thermal ellipsoids of **8** depicted at 50% probability. PPh_3 phenyl groups and hydrogen atoms, except for the N–H, are omitted for clarity. Selected bond distances (angstroms): Ru1–Cl1, 2.410(2); Ru1–Cl2, 2.411(2); Ru1–P1, 2.384(2); Ru1–P2, 2.371(2); Ru1–N1, 2.088(7); Ru1–N2, 2.092(8); N2–C7, 1.29(1); N3–C7, 1.38(1); N3–C14, 1.40(1); and N4–C14, 1.28(1).

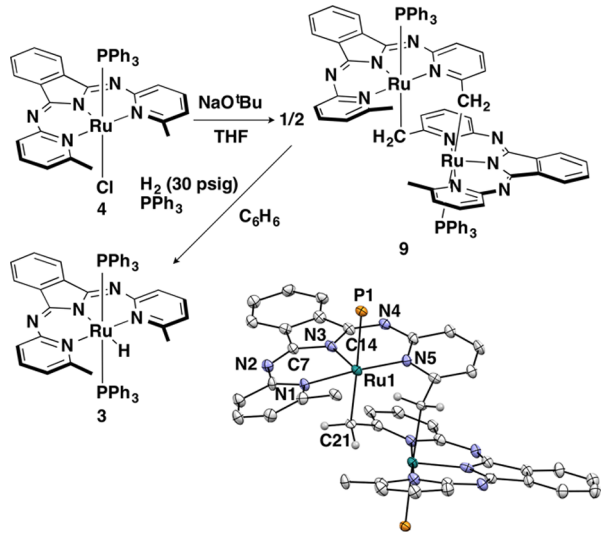

Figure 11. Synthesis of complex **9** and thermal ellipsoids of **9** depicted at 50% probability. PPh_3 phenyl groups and hydrogen atoms, except for the methanide, are omitted for clarity. Selected bond distances (angstroms): Ru1–P1, 2.392(1); Ru1–N1, 2.128(4); Ru1–N3, 1.968(4); Ru1–N5, 2.027(4); Ru1–C21, 2.221(5); N2–C7, 1.300(6); N3–C7, 1.371(8); N3–C14, 1.385(5); and N4–C14, 1.302(7).

experiment were obtained from slow evaporation of a DCM solution of **8** at 5 °C. The solid-state structure exposes an octahedral geometry around the Ru^{II} center, supported by a κ^2-HbMepi, two PPh_3 and two chloride ligands. Addition of 1.05 equiv of NaO^{t}Bu to a THF solution containing **8** cleanly afforded complex **4**, which is a benchtop-stable precatalyst in the base-promoted AAD reaction.

Isolation of an Alternative Promoterless AAD Catalyst. In (de)hydrogenation catalysis, active Ru complexes are often generated using exogenous base additives.[41] We previously showed that **4** was activated in the presence of NaO^{t}Bu to provide an active dehydrogenation catalyst; however, the mechanism of activation was unclear. Stoichiometric reactions between **4** and base were performed to examine the reaction pathway. Under basic conditions, deprotonation of the *ortho*-methyl group was achieved by $^-$O^{t}Bu base, and the deprotonated intermediate was subsequently trapped by coordination with another Ru complex to afford a dimer (**9**), which was isolated in 78% yield (Figure 11). Crystals suitable for single-crystal X-ray diffraction were obtained from vapor diffusion of pentane into a benzene solution of **9**, and the solid-state structure reveals a square-based pyramidal geometry about the Ru center (τ = 0.02, 0.03)[22] with the pincer ligand meridionally coordinated and the pyridinylmethanide motif coordinated to another Ru^{II} center (Figure 11). The asymmetry of the pincer ligand is confirmed in solution by >10 distinct resonances in the aromatic region of the ^{1}H NMR spectrum.

To investigate complex **9** as a precursor en route to the catalytically active HRu(bMepi)(PPh_3) species, a reaction with H_2 was examined. H_2 was heterolytically cleaved by the pyridinylmethanide group and the Ru center at low pressure (30 psig) and reacted with another PPh_3 molecule to afford **3** (Figure 11). This demonstrates that complex **9** is a precursor to the HRu(bMepi)(PPh_3) species and that the methanide motif is an internal basic site that may promote dehydrogenation reactions without requiring any additives. To illustrate the latter point, refluxing a 0.25 M 1PhEtOH toluene solution containing 0.5 mol % **9** for 4 h resulted in quantitative conversion (>99%) of 1PhEtOH to acetophenone (eq 15). Hence, complex **9** is a precursor to generate a catalytically active HRu(bMepi)(PPh_3) species that operates via the AAD catalytic cycle proposed in Scheme 10.

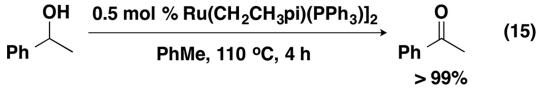

Reversible Catalytic Hydrogenation–Dehydrogenation Reactions. Catalytic hydrogenation and dehydrogenations reactions are attractive candidates to target for reversible energy storage.[2,42] Although a myriad of catalysts can mediate the forward *or* reverse reaction, very few systems are capable of catalyzing reversible hydrogenation–dehydrogenation reactions.[2a,7,43] The ability of **3** to effect a catalytic transfer hydrogenation reaction using ^{i}PrOH as the H_2 surrogate was previously demonstrated.[8] Thus, we hypothesized that the hydrogenation reactions should be possible using H_2 given that entry to **3** was also gained by treating the Ru-alkoxide (**6**) with H_2. Indeed, acetophenone was completely consumed to afford 1PhEtOH within 1 h at 110 °C using 1 mol % **3** and 30 psig H_2 in PhMe-d_8 inside a J. Young NMR tube. Following the hydrogenation reaction, the solution was transferred from the J. Young NMR tube to a Schlenk flask to assess the ability to promote the dehydrogenation of 1PhEtOH. Refluxing the toluene solution under an inert atmosphere for 4 h restored acetophenone quantitatively (Scheme 14). This demonstrates the complete and reversible transformations between acetophenone and 1PhEtOH via successive hydrogenation–dehydrogenation reactions using complex **3** as the *single* catalyst.

CONCLUSION

The mechanism of the AAD reaction catalyzed by complex **3** was studied by a series of kinetic and isotopic labeling experiments, isolation of intermediates, and catalyst modifications. Experimental evidence supported an inner-sphere,

DOI: 10.1021/acscatal.5b00952
ACS Catal. 2015, 5, 5468–5485

Scheme 14. Reversible Hydrogenation−Dehydrogenation Reactions Catalyzed by 3

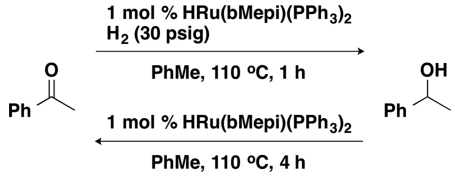

stepwise pathway for proton and hydride transfers with a β-H elimination turnover-limiting step. Selective isotopic labeling experiments combined with catalyst modification (methylation of the pincer ligand backbone) demonstrated that a cooperative metal−ligand pathway involving the imine functionality is not necessary for efficient dehydrogenation. The activation parameters suggested an associative pathway involving a highly ordered transition-state structure. Thus, we propose that a single PPh_3 dissociation event from **3** generates a coordinatively unsaturated HRu(bMepi)(PPh_3) species, which undergoes a proton-transfer equilibrium to generate a transient Ru-(H_2) alkoxide species. H_2 loss affords a Ru-alkoxide intermediate that can participate in a turnover-limiting β-H elimination reaction to complete the catalytic cycle (Scheme 15). Moreover, modifications to the pincer ligand revealed that the steric profiles of the methyl groups on bMepi slightly impeded catalytic activity, while electronic modifications of the pincer ligand have a minimal effect on the rate of catalytic dehydrogenation.

In addition to delineating a detailed mechanistic understanding of dehydrogenative catalysis mediated by **3**, we also showed **3** as an efficient hydrogenation precatalyst. By coupling the hydrogenation and the dehydrogenation abilities of **3**, we have thus demonstrated that completely reversible transformations between ketones and alcohols are achieved and are dictated by hydrogen input or release. Overall, such reversible catalytic reactions are of broad interest to the field of hydrogen storage as well as chemical synthesis.

EXPERIMENTAL SECTION

General Considerations. All manipulations were conducted under a nitrogen atmosphere on a Schlenk manifold or in a glovebox using standard Schlenk techniques, unless otherwise stated. All reagents were purchased from commercial vendors. Anhydrous dichloroethane (DCE, Acros), NaO^{t}Bu (Sigma-Aldrich), and MeOTf (Sigma-Aldrich) were used without further purification. 1-Phenylethanol, phenyltrimethylsilane, acetophenone, 1-(4-methylphenyl)ethanol, 1-(4-methoxyphenyl)ethanol, 1-(4-fluorophenyl)ethanol, 1PhEtOD, 1PhCH$_3$CDOH, 1PhCH$_3$CDOD, and 2,2,2-trifluoroethanol were distilled from CaH_2 under a nitrogen atmosphere and then stored over 3 Å molecular sieves for at least 24 h. The following compounds were synthesized according to literature methods: HRu(bMepi)(PPh_3)$_2$ (**3**),[8] Ru(bMepi)(PPh_3)Cl

Scheme 15. Proposed Cycle for Catalytic AAD and Isolation of Precursors

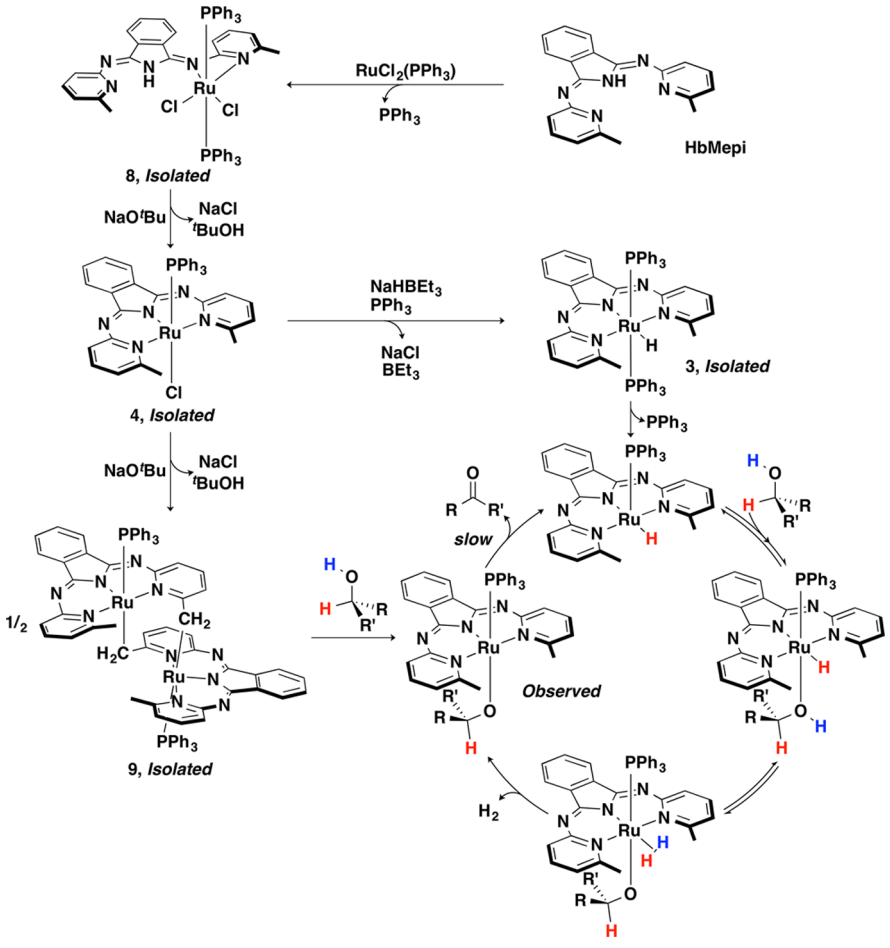

DOI: 10.1021/acscatal.5b00952
ACS Catal. 2015, 5, 5468−5485

(4),[8] 1PhEtOH isotopologues,[19] and the Hb4Rpi ligands.[44] The 3 Å molecular sieves were dried at 250 °C under dynamic vacuum for 24 h. Dichloromethane (DCM), diethyl ether (Et_2O), pentane, benzene (C_6H_6), dimethoxyethane (DME), and tetrahydrofuran (THF) were purified using a Glass Contour solvent purification system consisting of a copper catalyst, neutral alumina, and activated molecular sieves then passed through an in-line, 2 μm filter immediately before being dispensed. Toluene (PhMe) and hexanes (Hex) were sparged using nitrogen and then stored over 3 Å molecular sieves for at least 24 h.

NMR spectra were recorded on Varian Inova 500, Varian MR400, Varian vnmrs 500, and Varian vnmrs 700 spectrometers at ambient temperature. ^{1}H and ^{13}C shifts are reported in parts per million (ppm) relative to TMS, with the residual solvent peak used as an internal reference. ^{31}P and ^{19}F NMR spectra were referenced on a unified scale to their respective ^{1}H NMR spectra. At elevated temperatures, ^{31}P spectra were referenced relative to an internal standard of PPh_3 at −5.6 ppm. The following abbreviations are reported as follows: singlet (s), doublet (d), doublet of doublets (dd), triplet (t), quartet (q), multiplet (m), methyl (Me), methoxy (OMe), and triphenylphosphine (PPh_3). ^{13}C NMR resonances were observed as singlets unless otherwise stated. For atom numbering of the bpi ligand in complexes **4**−**7**, see Figure 12.

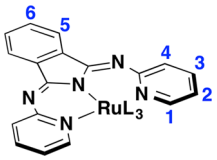

Figure 12. Atom numbering of the bpi ligand for the NMR characterization of **4**−**7**.

Solid-state IR spectra were collected using a Nicolet iS10 spectrometer equipped with a diamond attenuated total reflectance (ATR) accessory. Elemental analyses were performed by Midwest Microlab, LLC.

General Procedure for 1PhEtOH Dehydrogenation Catalyzed by 3. 1PhEtOH (5 mL, 41.4 mmol) was added to a 20 mL vial charged with **3** (3.9 mg, 0.00409 mmol), PhTMS (0.5 mL, 2.9 mmol), and a stir bar. The vial was capped with a septum and pierced with a 27-gauge needle. Then the vial was heated to the desired temperature (90, 100, 110, 120, or 130 °C) using an aluminum heating block inside an inert-atmosphere glovebox. The formation of acetophenone was monitored by sampling 0.5 mL aliquots and then analyzed by ^{1}H NMR spectroscopy against PhTMS as an internal standard. To confirm reproducibility, all kinetic experiments were performed in triplicate.

General Procedure for Base-Promoted 1PhEtOH Dehydrogenation. PhMe (2 mL) was added to a 10 mL Schlenk flask charged with [Ru] (0.005 mmol; **4**, 3.6 mg; **5**, 5.0 mg; $RuCl_2(PPh_3)_3$, 4.8 mg; and HbMepi, 1.6 mg), NaO^{t}Bu (2 mol %, 0.01 mmol, 1.0 mg; 3 mol %, 0.015 mmol, 1.4 mg), and a stir bar. 1PhEtOH (60 μL, 0.5 mmol) was added to the mixture. A reflux condenser was connected to the Schlenk flask, capped with a septum, and pierced with a 27-gauge needle in addition to a nitrogen inlet 16-gauge needle. The reaction solution was heated to 120 °C using an aluminum heating block. After 4 h, the reaction mixture was cooled to ambient temperature and exposed to air to quench the reaction. The solvent was evaporated under vacuum, and the residue was purified through a plug of silica gel eluting with Et_2O (5 mL). Evaporation of the Et_2O solution afforded acetophenone as a colorless oil. The purity and identity were confirmed by comparison to previously reported NMR data.

Ru(HbMepi)(PPh$_3$)Cl[PF$_6$]. THF (3 mL) was added to a vial charged with HbMepi (51.6 mg, 0.158 mmol), $RuCl_2(PPh_3)_3$ (137.4 mg, 0.143 mmol), $TlPF_6$ (50.1 mg, 0.143 mmol), and a stir bar. The reaction solution was allowed to stir at 70 °C for 2 days. After the solution was cooled to ambient temperature, TlCl was filtered using a fine frit and the THF solvent was removed under vacuum. The crude product was washed with C_6H_6 (4 × 10 mL) and Et_2O (4 × 10 mL). The crude product was dissolved in minimum DCM and layered with Et_2O. After 24 h at ambient temperature, the precipitates were collected and washed with Et_2O (4 × 10 mL). Evaporation of the volatiles under vacuum afforded the product as a dark blue solid. Crystals were obtained from vapor diffusion of Et_2O into a DCM solution at ambient temperature. Yield: 94 mg (75%). ^{1}H NMR (700 MHz, CD_2Cl_2): δ 10.85 (s, 1H, NH), 8.17 (t, J_{HH} = 7.0 Hz, 1H), 7.94 (d, J_{HH} = 7.7 Hz, 1H), 7.69 (d, J_{HH} = 5.6 Hz, 1H) 7.62 (bs, 1H), 7.51 (bs, 1H), 7.45−7.44 (m, 2H), 7.34 (d, J_{HH} = 7.0 Hz, 1H), 7.27 (bs, 1H), 7.17 (t, J_{HH} = 7.0 Hz, 3H, PPh_3), 6.92 (t, J_{HH} = 7.0 Hz, 6H, PPh_3), 6.52 (t, J_{HH} = 9.1 Hz, 6H, PPh_3), 1.78 (s, 3H, Me), 1.70 (s, 3H, Me). ^{13}C{^{1}H} (176 MHz, CD_2Cl_2): δ 160.99, 160.90, 156.363, 153.37, 147.34, 146.49, 139.11, 138.98, 138.57, 132.71, 132.58, 132.53, 131.93, 131.04, 130.86, 129.65, 129.13, 129.08, 124.43, 123.46, 122.55, 121.30, 115.64, 23.56, 22.76. ^{31}P{^{1}H} NMR (162 MHz, CD_2Cl_2): δ 39.17 (s, PPh_3), −144.30 (septet, J_{PF} = 710 Hz, PF_6). ^{19}F NMR (376 MHz, CD_2Cl_2): δ −72.77 (d, J_{FP} = 710 Hz, PF_6). IR (ATR, cm^{-1}): 3331, 3059, 1631, 1600, 1552, 1532, 1463, 1449, 1433, 1372, 1292, 1210, 1163, 1104, 1088, 998, 833, 795, 740, 692. Anal. Calculated (found): C, 52.39 (52.51); H, 3.70 (3.80); N, 8.04 (7.85).

Preparation of Ru(bMepi)(PPh$_3$)Cl (4) from Ru(HbMepi)(PPh$_3$)Cl[PF$_6$]. THF (5 mL) was added to a 20 mL vial charged with Ru(HbMepi)(PPh_3)Cl[PF_6] (10 mg, 0.0115 mmol), NaO^{t}Bu (1.1 mg, 0.0115 mmol), and a stir bar. The reaction solution was allowed to stir at ambient temperature for 30 min. Solvent was removed under vacuum, and the crude product was extracted with DCM (10 mL). The DCM solvent was removed under vacuum, and the product was washed with Et_2O (4 × 10 mL). Evaporation of the volatiles under vacuum afforded the product as a dark purple powder. The purity and identity were confirmed by comparison to previously reported NMR data. Yield: 7.5 mg (90%).

*Ru(b4,6-Mepi)(PPh$_3$)Cl (**4-CH$_3$**).* THF (10 mL) was added to a 20 mL vial charged with Kb4,6-Mepi (103.7 mg, 0.264 mmol), $RuCl_2(PPh_3)_3$ (240.6 mg, 0.251 mmol), and a stir bar. The resulting solution was stirred at room temperature for 17 h. Solvent was removed under vacuum. The crude product was washed with Et_2O (4 × 5 mL) and extracted with DCM (4 × 5 mL). The DCM solvent was removed under vacuum, and the product was washed with pentane (4 × 10 mL), affording the product as a dark blue powder. The product was recrystallized from layering pentane on top of a DCM solution at −35 °C. Yield: 126 mg (68%). ^{1}H NMR (400 MHz, C_6D_6): δ 7.98 (dd, J_{HH} = 5.6, 3.2 Hz, 2H, H^5), 7.51 (s, 2H, H^4), 7.05 (dd, J_{HH} = 5.2, 2.8 Hz, 2H, H^6), 6.86 (t, J_{HH} = 8.4 Hz, 6H, PPh_3), 6.77 (t, J_{HH} = 7.2 Hz, 3H, PPh_3), 6.67 (t, J_{HH} = 6.8 Hz, 6H, PPh_3), 6.24 (s, 2H, H^2), 1.98 (s, 6H, *p*-Me), 1.78 (s, 6H, *o*-Me). ^{13}C{^{1}H} (176 MHz, CD_2Cl_2): δ 158.69, 154.87, 153.30, 147.36, 141.48,

DOI: 10.1021/acscatal.5b00952
ACS Catal. 2015, 5, 5468−5485

134.26, 134.03, 133.01, 129.53, 128.92, 128.20, 125.82, 121.44, 119.96. $^{31}P\{^{1}H\}$ NMR (162 MHz, C_6D_6): δ 45.34 (s, PPh_3). IR (ATR, cm^{-1}): 3052, 1622, 1566, 1498, 1447, 1430, 1372, 1327, 1289, 1251, 1229, 1204, 1182, 1109, 1087, 1030, 1001, 969, 900, 843, 773, 745, 726, 694. Anal. Calculated (found): C, 63.78 (63.59); H, 4.68 (4.48); N, 9.30 (9.17).

*Ru(bMepi^{Me})(PPh$_3$)(OTf)$_2$ (**5**).* MeOTf (150 μL, 1.39 mmol) was added to a 20 mL vial containing DCM solution of **4** (101 mg, 0.139 mmol) and a stir bar. The reaction solution was allowed to stir at ambient temperature for 16 h. The DCM solvent was removed under vacuum, and the crude product was washed with Et_2O (4 × 10 mL). The crude product was dissolved in minimum DCM and layered with Et_2O. After 24 h at ambient temperature, the precipitates were collected and washed with Et_2O (4 × 10 mL). Evaporation of the volatiles under vacuum afforded the product as a dark purple crystalline solid. Crystals were obtained from vapor diffusion of pentane into a DCM/C_6H_6 solution at ambient temperature. Yield: 111 mg (79%). ^{1}H NMR (500 MHz, CD_2Cl_2): δ 8.30−8.27 (m, 2H), 8.13 (t, J_{HH} = 7.5 Hz, 1H), 7.95 (d, J_{HH} = 8.0 Hz, 1H), 7.83−7.80 (m, 2H), 7.72−7.65 (m, 2H), 7.39−7.35 (m, 5H), 7.14 (t, J_{HH} = 8.0 Hz, 6H, PPh_3), 6.81 (t, J_{HH} = 10.5 Hz, 6H, PPh_3), 3.73 (s, 3H, N-Me), 1.78 (s, 3H, Me), 1.57 (s, 3H, Me). $^{13}C\{^{1}H\}$ (176 MHz, CD_2Cl_2): δ 165.67, 160.83, 160.25, 153.97, 152.62, 148.97, 141.13, 140.89, 139.70, 134.86, 132.81, 132.76, 132.39, 131.55, 131.05, 130.77, 129.55, 129.49, 124.94, 124.59, 124.44, 123.76, 116.42, 44.46, 22.97, 21.76. $^{31}P\{^{1}H\}$ NMR (202 MHz, CD_2Cl_2): δ 47.84 (s, PPh_3). IR (ATR, cm^{-1}): 3062, 1609, 1565, 1519, 1459, 1435, 1400, 1308, 1266, 1230, 1206, 1187, 1156, 1117, 1090, 1015, 909, 811, 797, 779, 742, 696. Anal. Calculated (found): C, 49.10 (48.97); H, 3.42 (3.51); N, 6.98 (6.88).

*Ru(bMepi)(PPh$_3$)(OCH$_2$CF$_3$) (**6**).* CF_3CH_2OH (4.3 μL, 0.0563 mmol) was added to a 20 mL vial containing THF solution of **3** (48.8 mg, 0.051 mmol) and a stir bar. The reaction solution was allowed to stir at 70 °C for 2 days. After cooling to ambient temperature, the THF solvent was removed under vacuum and the crude product was washed with Et_2O (4 × 10 mL) and pentane (4 × 10 mL). The product was extracted with C_6H_6 (15 mL). The C_6H_6 solution was lyophilized, affording the product as a purple powder. Crystals were obtained from vapor diffusion of pentane into a PhMe solution at 5 °C. Yield: 22 mg (55%). ^{1}H NMR (700 MHz, C_6D_6): δ 8.09 (dd, J_{HH} = 5.6, 3.5 Hz, 2H, H^5), 7.69 (d, J_{HH} = 7.7 Hz, 2H, H^4), 7.19 (t, J_{HH} = 7.7 Hz, 2H, H^3), 7.06 (dd, J_{HH} = 5.6, 2.8 Hz, 2H, H^6), 6.77−6.72 (m, 9H, PPh_3), 6.65 (t, J_{HH} = 7.0 Hz, 6H), 6.35 (d, J_{HH} = 7.0 Hz, 2H, H^2), 3.28 (q, J_{HF} = 7.7, J_{HH} = 2.1 Hz, 2H, OCH_2CF_3), 1.75 (s, 6H, Me). $^{13}C\{^{1}H\}$ (176 MHz, C_6D_6): δ 159.69, 155.41, 152.68, 142.22, 136.03, 135.83, 134.59, 132.92, 132.86, 125.59, 120.31, 118.69, 67.59, 23.48. $^{31}P\{^{1}H\}$ NMR (283 MHz, PhMe-d_8): δ 43.88 (s, PPh_3). $^{19}F\{^{1}H\}$ NMR (376 MHz, PhMe-d_8) δ −76.52 (s, OCH_2CF_3). IR (ATR, cm^{-1}): 3041, 2814, 2714, 1568, 1538, 1512, 1460, 1433, 1388, 1264, 1184, 1153, 1121, 1107, 1009, 949, 905, 794, 769, 742, 693. Anal. Calculated (found): C, 60.91 (60.88); H, 4.22 (4.29); N, 8.88 (8.63).

*Ru(bpi)(PPh$_3$)$_2$Cl (**7-H**).* THF (15 mL) was added to a 20 mL vial charged with Hbpi (319.4 mg, 1.07 mmol), $RuCl_2(PPh_3)_3$ (974.4 mg, 1.02 mmol), $TlPF_6$ (355 mg, 1.02 mmol), and a stir bar. The reaction solution was allowed to stir at 70 °C for 21 h. After cooling to ambient temperature, TlCl was filtered using a fine frit and the THF solvent was removed under vacuum. The crude product was washed with Et_2O (4 × 20 mL), affording Ru(Hbpi)$(PPh_3)_2Cl[PF_6]$ in 83% yield (932 mg). THF (15 mL) was added to a 20 mL vial charged with Ru(Hbpi)-$(PPh_3)_2Cl[PF_6]$ (925.5 mg, 0.837 mmol), NaO^{t}Bu (84.5 mg, 0.879 mmol), and a stir bar. The reaction solution was allowed to stir at ambient temperature for 30 min. The THF solvent was removed under vacuum, and the crude product was extracted with C_6H_6 (50 mL). The C_6H_6 solution was lyophilized, and the product was washed with pentane (4 × 20 mL). Evaporation of the volatiles under vacuum afforded the product as a green powder. Crystals were obtained from slow evaporation of a DCM solution at ambient temperature (DCM/Hex). Yield: 562 mg (70%). ^{1}H NMR (400 MHz, C_6D_6): δ 10.60 (d, J_{HH} = 6.4 Hz, 2H, H^1), 7.95 (dd, J_{HH} = 4.8, 2.4 Hz, 2H, H^5), 7.37−7.33 (m, 14H), 6.88 (t, J_{HH} = 8.4 Hz, 2H, H^3), 6.81−6.71 (m, 18H), 6.00 (t, J_{HH} = 8.8 Hz, 2H, H^2). $^{13}C\{^{1}H\}$ (176 MHz, CD_2Cl_2): δ 158.47, 157.43, 152.63, 141.83, 134.43, 133.89, 132.69 (t, J_{CP} = 17.2 Hz, *ipso*-CP), 128.86, 128.56, 127.59, 127.21, 119.93, 116.59. $^{31}P\{^{1}H\}$ NMR (162 MHz, C_6D_6): δ 26.09 (s, PPh_3). IR (ATR, cm^{-1}): 3053, 1568, 1552, 1513, 1454, 1434, 1378, 1305, 1290, 1210, 1186, 1105, 1087, 1007, 909, 843, 770, 744, 696. Anal. Calculated (found): C, 67.60 (67.25); H, 4.41 (4.40); N, 7.30 (7.20).

*Ru(b4Mepi)(PPh$_3$)$_2$Cl (**7-Me**).* THF (10 mL) was added to a 20 mL vial charged with Hb4Mepi (103.7 mg, 0.317 mmol), $RuCl_2(PPh_3)_3$ (303.7 mg, 0.317 mmol), $TlPF_6$ (110.7 mg, 0.317 mmol), and a stir bar. The reaction solution was allowed to stir at 60 °C for 24 h. After the solution cooled to ambient temperature, TlCl was filtered using a fine frit and the THF solvent was removed under vacuum. The crude product was washed with Et_2O (4 × 10 mL), affording Ru(Hb4Mepi)-$(PPh_3)_2Cl[PF_6]$ in 87% yield (312 mg). THF (15 mL) was added to a 20 mL vial charged with Ru(Hb4Mepi)$(PPh_3)_2Cl$-$[PF_6]$ (122 mg, 0.108 mmol), NaO^{t}Bu (10.9 mg, 0.113 mmol), and a stir bar. The reaction solution was allowed to stir at ambient temperature for 30 min. The THF solvent was removed under vacuum, and the crude product was extracted with C_6H_6. The C_6H_6 solution was lyophilized, and the product was washed with pentane (4 × 10 mL). Evaporation of the volatiles under vacuum afforded the product as a green powder. Crystals were obtained from layering pentane on top of a DCM solution at −35 °C. Yield: 90 mg (85%). ^{1}H NMR (400 MHz, C_6D_6): δ 10.44 (d, J_{HH} = 6.4 Hz, 2H, H^1), 7.98 (dd, J_{HH} = 5.2, 2.8 Hz, 2H, H^5), 7.44−7.39 (m, 12H, PPh_3), 7.26 (s, 2H, H^4), 6.81−6.73 (m, 18H, PPh_3), 5.92 (d, J_{HH} = 6.8 Hz, 2H, H^2), 1.76 (s, 6H, Me). $^{13}C\{^{1}H\}$ (176 MHz, CD_2Cl_2): δ 157.44, 156.94, 152.95, 145.93, 141.85, 133.96, 133.08 (t, J_{CP} = 17.0 Hz, *ipso*-CP), 128.72, 128.45, 127.49, 119.75, 118.50. $^{31}P\{^{1}H\}$ NMR (162 MHz, C_6D_6): δ 26.14 (s, PPh_3). IR (ATR, cm^{-1}): 3053, 1552, 1501, 1481, 1462, 1431, 1403, 1375, 1293, 1189, 1102, 1088, 1007, 941, 840, 817, 746, 693. Anal. Calculated (found): C, 68.11 (68.38); H, 4.70 (4.79); N, 7.09 (6.99).

*Ru(b4Clpi)(PPh$_3$)$_2$Cl (**7-Cl**).* THF (10 mL) was added to a 20 mL vial charged with Hb4Clpi (88 mg, 0.239 mmol), $RuCl_2(PPh_3)_3$ (218.2 mg, 0.228 mmol), $TlPF_6$ (79.5 mg; 0.228 mmol), and a stir bar. The reaction solution was allowed to stir at 60 °C for 18 h. After the solution cooled to ambient temperature, TlCl was filtered using a fine frit and the THF solvent was removed under vacuum. The crude product was washed with Et_2O (4 × 10 mL), affording Ru(Hb4Clpi)-$(PPh_3)_2Cl[PF_6]$ in 91% yield (242 mg). THF (10 mL) was added to a 20 mL vial charged with Ru(Hb4Clpi)$(PPh_3)_2Cl$-$[PF_6]$ (242 mg, 0.206 mmol), NaO^{t}Bu (20.8 mg, 0.216 mmol),

DOI: 10.1021/acscatal.5b00952
ACS Catal. 2015, 5, 5468−5485

and a stir bar. The reaction solution was allowed to stir at ambient temperature for 30 min. The THF solvent was removed under vacuum, and the crude product was extracted with C_6H_6. The C_6H_6 solution was lyophilized, and the product was washed with pentane (4 × 10 mL). Evaporation of the volatiles under vacuum afforded the product as a green powder. Yield: 131 mg (62%). ^{1}H NMR (700 MHz, CD_2Cl_2): δ 9.87 (d, J_{HH} = 7.0 Hz, 2H, H^1), 7.60 (dd, J_{HH} = 5.6, 2.8 Hz, 2H, H^5), 7.39 (dd, J_{HH} = 5.6, 2.8 Hz, 2H, H^6), 7.17 (d, J_{HH} = 2.1 Hz, H^4), 7.07 (t, J_{HH} = 7.0 Hz, 6H, PPh_3), 6.94−6.88 (m, 24H, PPh_3), 6.27 (dd, J_{HH} = 7.0, 2.8 Hz, 2H, H^2). ^{13}C{^{1}H} (176 MHz, CD_2Cl_2): δ 158.61, 157.72, 153.38, 141.84, 141.55, 133.84, 132.46 (t, J_{CP} = 17.5 Hz, *ipso*-CP), 129.11, 129.02, 127.72, 126.49, 120.25, 116.92. ^{31}P{^{1}H} NMR (162 MHz, C_6D_6): δ 25.13 (s, PPh_3). IR (ATR, cm^{-1}): 3056, 1544, 1514, 1492, 1446, 1372, 1318, 1299, 1210, 1186, 1121, 1089, 1001, 914, 887, 868, 808, 776, 737, 694. Anal. Calculated (found): C, 63.07 (62.64); H, 3.92 (4.02); N, 6.81 (6.63).

*Ru(b4OMepi)(PPh$_3$)$_2$Cl (**7-OMe**).* THF (10 mL) was added to a 20 mL vial charged with Hb4OMepi (99 mg, 0.276 mmol), $RuCl_2(PPh_3)_3$ (251.6 mg, 0.262 mmol), $TlPF_6$ (91.7 mg, 0.262 mmol), and a stir bar. The reaction solution was allowed to stir at 60 °C for 16 h. After the solution cooled to ambient temperature, TlCl was filtered using a fine frit and the THF solvent was removed under vacuum. The crude product was washed with Et_2O (4 × 10 mL), affording Ru(Hb4OMepi)-$(PPh_3)_2Cl[PF_6]$ in 87% yield (267 mg). THF (10 mL) was added to a 20 mL vial charged with Ru(Hb4OMepi)$(PPh_3)_2$Cl-$[PF_6]$ (264 mg, 0.227 mmol), NaO^{t}Bu (22.9 mg, 0.238 mmol), and a stir bar. The reaction solution was allowed to stir at ambient temperature for 30 min. The THF solvent was removed under vacuum, and the crude product was extracted with C_6H_6. The C_6H_6 solution was lyophilized and the product was washed with pentane (4 × 10 mL). Evaporation of the volatiles under vacuum afforded the product as a dark blue powder. Yield: 192 mg (83%). ^{1}H NMR (400 MHz, C_6D_6): δ 10.32 (d, J_{HH} = 7.2 Hz, 2H, H^1), 7.99 (dd, J_{HH} = 5.6, 3.2 Hz, 2H, H^5), 7.50−7.46 (m, 12H, PPh_3), 6.99 (d, J_{HH} = 2.8 Hz, 2H, H^4), 6.79−6.78 (m, 18H, PPh_3), 5.86 (dd, J_{HH} = 7.2, 3.2 Hz, 2H, H^2), 3.10 (s, 6H). ^{13}C{^{1}H} (176 MHz, CD_2Cl_2): δ 165.35, 158.46, 158.10, 153.57, 141.82, 133.99, 133.23 (t, J_{CP} = 16.6 Hz, *ipso*-CP), 128.76, 128.57, 127.55, 119.76, 109.69, 106.69, 55.76. ^{31}P{^{1}H} NMR (162 MHz, C_6D_6): δ 26.40 (s, PPh_3). IR (ATR, cm^{-1}): 3050, 1619, 1558, 1509, 1467, 1436, 1378, 1328, 1178, 1091, 1039, 1002, 845, 744, 694. Anal. Calculated (found): C, 65.98 (65.45); H, 4.55 (4.44); N, 6.87 (6.86).

*Ru(b4OHpi)(PPh$_3$)$_2$Cl (**7-OH**).* THF (10 mL) was added to a 20 mL vial charged with Hb4OHpi (63.6 mg, 0.192 mmol), $RuCl_2(PPh_3)_3$ (184.1 mg, 0.192 mmol), NaO^{t}Bu (19.4 mg, 0.202 mmol), and a stir bar. The reaction solution was allowed to stir at 70 °C for 16 h. After the solution was cooled to ambient temperature, the THF solvent was removed under vacuum. The crude product was washed with DCM (4 × 10 mL), H_2O (4 × 10 mL), and Et_2O (4 × 10 mL). Evaporation of the volatiles under vacuum afforded the product as a dark blue powder. Crystals were obtained from vapor diffusion of pentane into a THF solution at −35 °C. Yield: 151 mg (79%). ^{31}P{^{1}H} NMR (162 MHz, THF): δ 26.40 (s, PPh_3). IR (ATR, cm^{-1}): 3046, 1555, 1517, 1478, 1432, 1324, 1296, 1186, 1103, 1091, 1017, 972, 912, 862, 795, 744, 693. Anal. Calculated (found): C, 65.42 (65.45); H, 4.27 (4.13); N, 7.06 (7.12).

*Ru(HbMepi)(PPh$_3$)$_2$Cl$_2$ (**8**).* DCE (5 mL) was added to a vial charged with HbMepi (51.2 mg, 0.156 mmol), $RuCl_2(PPh_3)_3$ (136.3 mg, 0.142 mmol), and a stir bar. The reaction solution was allowed to stir at ambient temperature for 24 h. The precipitate was collected on a frit and washed with Et_2O (4 × 10 mL), and the product was extracted with DCM. Evaporation of the volatiles under vacuum afforded the product as a green solid. Crystals were obtained from slow evaporation of a DCM solution at 5 °C (DCM/Hex). Yield: 113 mg (78%). ^{1}H NMR (400 MHz, CD_2Cl_2): δ 10.78 (s, 1H), 7.79 (d, J_{HH} = 7.6 Hz, 1H), 7.73−7.69 (m, 12H), 7.57 (t, J_{HH} = 7.6 Hz, 1H), 7.51 (t, J_{HH} = 7.6 Hz, 2H), 7.30 (t, J_{HH} = 7.8 Hz, 1H), 7.22 (t, J_{HH} = 7.8 Hz, 1H), 7.13−7.04 (m, 19H), 6.89 (d, J_{HH} = 7.6 Hz, 1H), 6.30 (d, J_{HH} = 8.0 Hz, 1H), 6.21 (d, J_{HH} = 8.0 Hz, 1H), 2.31 (s, 3H, Me), 0.99 (s, 3H, Me). ^{13}C{^{1}H} (176 MHz, CD_2Cl_2): δ 159.83, 159.34, 148.76, 138.27, 136.19, 135.56, 135.02, 134.19, 131.71, 131.10, 130.14, 129.86, 129.17, 128.76, 127.65, 127.09, 124.64, 123.27, 120.49, 118.49, 108.24, 24.23, 20.54. ^{31}P{^{1}H} NMR (162 MHz, CD_2Cl_2): δ 24.94 (s, PPh_3). IR (ATR, cm^{-1}): 3170, 3056, 1640, 1609, 1581, 1548, 1482, 1467, 1432, 1305, 1270, 1214, 1150, 1107, 1089, 1030, 1007, 805, 760, 748, 685, 655. Anal. Calculated (found): C, 65.69 (65.46); H, 4.63 (4.65); N, 6.84 (6.65).

*Dimer **9**.* THF (5 mL) was added to a 20 mL vial charged with **4** (110 mg, 0.152 mmol), NaO^{t}Bu (18.9 mg, 0.197 mmol), and a stir bar. The reaction solution was allowed to stir at ambient temperature for 18 h. The THF solvent was removed under vacuum, and the crude product was washed with pentane (4 × 20 mL) then extracted with C_6H_6. The C_6H_6 solution was lyophilized, and the product was washed with Et_2O (5 mL) and pentane (4 × 10 mL). Evaporation of the volatiles under vacuum afforded the product as a green powder. Crystals were obtained from vapor diffusion of pentane into a C_6H_6 solution at ambient temperature. Yield: 64 mg (62%). ^{1}H NMR (700 MHz, C_6D_6): δ 8.46 (t, J_{HH} = 7.0 Hz), 7.23−7.18 (m), 6.09−6.86 (m, PPh_3), 6.75−6.71 (m, PPh_3), 6.62−6.57 (m, PPh_3). Major species: 7.99 (d, J_{HH} = 7.7 Hz, 1H), 7.94 (d, J_{HH} = 7.0 Hz, 1H), 7.14 (t, J_{HH} = 7.0 Hz, 1H), 6.81 (d, J_{HH} = 7.7 Hz, 1H), 6.68 (t, J_{HH} = 7.7 Hz, 1H), 6.10 (d, J_{HH} = 7.0 Hz, 1H), 5.41 (d, J_{HH} = 7.7 Hz, 1H), 2.37 (t, J = 9.1 Hz, 1H), 1.78 (s, 3H, Me), −2.62 (t, J = 9.1 Hz, 1H). Minor species: 7.98 (d, J_{HH} = 7.0 Hz, 1H), 7.92 (d, J_{HH} = 7.7 Hz, 1H), 7.09−7.06 (m, 2H), 7.00 (d, J_{HH} = 7.7 Hz, 1H), 6.65 (t, J_{HH} = 7.7 Hz, 1H), 5.83 (d, J_{HH} = 7.0 Hz, 1H), 5.69 (d, J_{HH} = 7.7 Hz, 1H), 3.10 (t, J = 9.1 Hz, 1H), 0.70 (s, 3H, Me), −2.77 (t, J = 9.1 Hz, 1H). ^{13}C{^{1}H} (176 MHz, CD_2Cl_2): δ 174.34, 159.04, 157.10, 151.97, 150.29, 149.06, 142.89, 141.59, 134.77, 134.62, 133.51, 133.45, 133.13, 132.49, 126.08, 120.14, 119.67, 118.20, 116.30, 112.59, 27.60, 24.78, 20.37, 19.95. ^{31}P{^{1}H} NMR (283 MHz, C_6D_6): δ 33.05 (s, minor), 31.34 (s, major). IR (ATR, cm^{-1}): 3046, 2968, 2900, 2613, 1533, 1560, 1504, 1461, 1431, 1387, 1324, 1286, 1239, 1188, 1159, 1112, 1090, 1030, 998, 976, 903, 792, 764, 739, 693. Anal. Calculated (found): C, 66.27 (66.06); H, 4.39 (4.35); N, 10.17 (10.16).

■ ASSOCIATED CONTENT

Supporting Information

The Supporting Information is available free of charge on the ACS Publications website at DOI: 10.1021/acscatal.5b00952.

Kinetic plots and NMR spectra (PDF)

Chemical characterization (CIF)

DOI: 10.1021/acscatal.5b00952
ACS Catal. 2015, 5, 5468−5485

AUTHOR INFORMATION

Corresponding Author

*E-mail: nszym@umich.edu.

Notes

The authors declare no competing financial interest.

ACKNOWLEDGMENTS

We thank the anonymous reviewers for providing valuable suggestions during the submission process. Acknowledgment is made to the Donors of the American Chemical Society Petroleum Research Fund for support of this research (53760-DNI3), the University of Michigan Department of Chemistry, and the National Science Foundation (CHE-0840456) for X-ray instrumentation. N.K.S. is an Alfred P. Sloan Research Fellow and a Dow Corning Assistant Professor.

REFERENCES

(1) (a) Gunanathan, C.; Milstein, D. *Science* **2013**, *341*, 249−260. (b) Dobereiner, G. E.; Crabtree, R. H. *Chem. Rev.* **2010**, *110*, 681−703. (c) Friedrich, A.; Schneider, S. *ChemCatChem* **2009**, *1*, 72−73.

(2) (a) Bonitatibus, P. J.; Chakraborty, S.; Doherty, M. D.; Siclovan, O.; Jones, W. D.; Soloveichik, G. L. *Proc. Natl. Acad. Sci. U. S. A.* **2015**, *112*, 1687−1692. (b) Marr, A. C. *Catal. Sci. Technol.* **2012**, *2*, 279−287. (c) Johnson, T. C.; Morris, D. J.; Wills, M. *Chem. Soc. Rev.* **2010**, *39*, 81−88.

(3) Clapham, S. E.; Hadzovic, A.; Morris, R. H. *Coord. Chem. Rev.* **2004**, *248*, 2201−2237.

(4) Gunanathan, C.; Milstein, D. *Acc. Chem. Res.* **2011**, *44*, 588−602.

(5) (a) Li, H.; Wang, X.; Huang, F.; Lu, G.; Jiang, J.; Wang, Z.-X. *Organometallics* **2011**, *30*, 5233−5247. (b) Li, H.; Zheng, B.; Huang, K.-W. *Coord. Chem. Rev.* **2015**, *293−294*, 116−138.

(6) Zeng, G.; Sakaki, S.; Fujita, K.-i.; Sano, H.; Yamaguchi, R. *ACS Catal.* **2014**, *4*, 1010−1020.

(7) Zhang, G.; Vasudevan, K. V.; Scott, B. L.; Hanson, S. K. *J. Am. Chem. Soc.* **2013**, *135*, 8668−8681.

(8) Tseng, K.-N. T.; Kampf, J. W.; Szymczak, N. K. *Organometallics* **2013**, *32*, 2046−2049.

(9) Complex **3** and Ru(bMepi)(PPh_3)Cl (**4**) are now commercially available.

(10) See Figure S1.

(11) Mikhailine, A. A.; Maishan, M. I.; Lough, A. J.; Morris, R. H. *J. Am. Chem. Soc.* **2012**, *134*, 12266−12280.

(12) Concentrations higher than 20-fold excess of PPh_3 with respect to **3** are likely to have an effect on the dehydrogenation rate; however, those scenarios deviate greatly from the standard conditions (Scheme 4) and thus are not meaningful to obtaining relevant analysis on the AAD mechanism.

(13) The neat concentration of 1PhEtOH is 8.3 M. Low 1PhEtOH concentrations are operationally challenging because replacing 1PhEtOH impacts other factors, such as dielectric constant, solvation, and polarizability, which influence the kinetic studies and the AAD mechanism.

(14) Morse, P. M.; Spencer, M. D.; Wilson, S. R.; Girolami, G. S. *Organometallics* **1994**, *13*, 1646−1655.

(15) Wilkins, R. G. *Kinetics and Mechanism of Reactions of Transition Metal Complexes*; Wiley-VCH: Weinheim, Germany, 2003; pp 199−256.

(16) Casey, C. P.; Singer, S. W.; Powell, D. R.; Hayashi, R. K.; Kavana, M. *J. Am. Chem. Soc.* **2001**, *123*, 1090−1100.

(17) (a) Mueller, J. A.; Goller, C. P.; Sigman, M. S. *J. Am. Chem. Soc.* **2004**, *126*, 9724−9734. (b) Blum, O.; Milstein, D. *J. Am. Chem. Soc.* **1995**, *117*, 4582−4594. (c) Martínez-Prieto, L. M.; Ávila, E.; Palma, P.; Álvarez, E.; Cámpora, J. *Chem. - Eur. J.* **2015**, *21*, 9833−9849.

(18) For further discussions of equilibrium isotope effects at transition-metal centers see: (a) Slaughter, L. M.; Wolczanski, P. T.; Klinckman, T. R.; Cundari, T. R. *J. Am. Chem. Soc.* **2000**, *122*, 7953−7975. (b) Janak, K. E.; Parkin, G. *J. Am. Chem. Soc.* **2003**, *125*, 6889−6891. (c) Gómez-Gallego, M.; Sierra, M. A. *Chem. Rev.* **2011**, *111*, 4857−4963.

(19) Johnson, J. B.; Bäckvall, J.-E. *J. Org. Chem.* **2003**, *68*, 7681−7684.

(20) Tseng, K.-N. T.; Kampf, J. W.; Szymczak, N. K. *ACS Catal.* **2015**, *5*, 411−415.

(21) Csonka, R.; Speier, G.; Kaizer, J. *RSC Adv.* **2015**, *5*, 18401−18419.

(22) Addison, A. W.; Rao, T. N.; Reedijk, J.; van Rijn, J.; Verschoor, G. C. *J. Chem. Soc., Dalton Trans.* **1984**, 1349−1356.

(23) Brookhart, M.; Green, M. L. H.; Parkin, G. *Proc. Natl. Acad. Sci. U. S. A.* **2007**, *104*, 6908−6914.

(24) The hydrogen atoms were refined assuming an idealized geometry for the sp^3 carbon; thus, the M−H distances are approximate values.

(25) An identical rate ($7.7(3) \times 10^{-5}$ M·s^{-1}) was obtained for **4** when 2 equiv of NaOTf was added, which suggests that the NaOTf generated when **5** was used had no effect on the catalytic rate of 1PhEtOH dehydrogenation.

(26) It should be noted that although the metal−ligand cooperative pathway was effectively turned off for **5**, this hybrid hydrogen-transfer mechanism may still be a plausible competing pathway for **3**.

(27) Kaneda, K.; Mori, K.; Hara, T.; Mizugaki, T.; Ebitani, K. *Catal. Surv. Asia* **2004**, *8*, 231−239.

(28) Vijayasri, K.; Rajaram, J.; Kuriacose, J. C. *J. Mol. Catal.* **1987**, *39*, 203−217.

(29) Thorson, M. K.; Klinkel, K. L.; Wang, J.; Williams, T. J. *Eur. J. Inorg. Chem.* **2009**, *2009*, 295−302.

(30) Fluorination has a destabilizing effect (15 kcal/mol) on the transition state for β-H elimination. See references: (a) Gellman, A. J.; Dai, Q. *J. Am. Chem. Soc.* **1993**, *115*, 714−722. (b) Johnson, T. J.; Huffman, J. C.; Caulton, K. G. *J. Am. Chem. Soc.* **1992**, *114*, 2725−2726.

(31) Further confirmation of the ruthenium alkoxide complex was not possible by 2D NMR correlation experiments, such as HMBC. For a discussion, see: *Phosphorous-31 NMR Spectroscopy*; Kuhl, O., Ed.; Springer: New York, 2008; pp 7−23.

(32) Ritter, J. C. M.; Bergman, R. G. *J. Am. Chem. Soc.* **1998**, *120*, 6826−6827.

(33) Blum, O.; Milstein, D. *J. Organomet. Chem.* **2000**, *593−594*, 479−484.

(34) For a recent example of large entropic factors in an unimolecular reaction performed in a protic solvent, see: Byers, J. A.; Jamison, T. F. *Proc. Natl. Acad. Sci. U. S. A.* **2013**, *110*, 16724−16729.

(35) For other examples demonstrating similar chemoselectivity see: (a) Chakraborty, S.; Lagaditis, P. O.; Förster, M.; Bielinski, E. A.; Hazari, N.; Holthausen, M. C.; Jones, W. D.; Schneider, S. *ACS Catal.* **2014**, *4*, 3994−4003. (b) Manzini, S.; Urbina-Blanco, C. A.; Nolan, S. P. *Organometallics* **2013**, *32*, 660−664.

(36) The standard enthalpy of formation in the gas phase for acetophenone and benzaldehyde are −87 and −37 kJ/mol, respectively. See http://webbook.nist.gov/chemistry/name-ser.html.

(37) Olmstead, W. N.; Margolin, Z.; Bordwell, F. G. *J. Org. Chem.* **1980**, *45*, 3295−3299.

(38) Golden, D. M.; Benson, S. W. *Chem. Rev.* **1969**, *69*, 125−134.

(39) Ellis, W. W.; Ciancanelli, R.; Miller, S. M.; Raebiger, J. W.; Rakowski DuBois, M.; DuBois, D. L. *J. Am. Chem. Soc.* **2003**, *125*, 12230−12236.

(40) Hansch, C.; Leo, A.; Taft, R. W. *Chem. Rev.* **1991**, *91*, 165−195.

(41) (a) Spasyuk, D.; Smith, S.; Gusev, D. G. *Angew. Chem., Int. Ed.* **2012**, *51*, 2772−2775. (b) He, L.-P.; Chen, T.; Gong, D.; Lai, Z.; Huang, K.-W. *Organometallics* **2012**, *31*, 5208−5211. (c) Wang, Z.; Belli, J.; Jensen, C. M. *Faraday Discuss.* **2011**, *151*, 297−305. (d) Nielsen, M.; Kammer, A.; Cozzula, D.; Junge, H.; Gladiali, S.; Beller, M. *Angew. Chem., Int. Ed.* **2011**, *50*, 9593−9597.

(42) (a) Grellier, M.; Sabo-Etienne, S. *Dalton Trans.* **2014**, *43*, 6283−6286. (b) Crabtree, R. H. *Energy Environ. Sci.* **2008**, *1*, 134−138.

(43) (a) Chakraborty, S.; Brennessel, W. W.; Jones, W. D. *J. Am. Chem. Soc.* **2014**, *136*, 8564−8567. (b) Fujita, K.-i.; Tanaka, Y.;

DOI: 10.1021/acscatal.5b00952
ACS Catal. 2015, 5, 5468−5485

Kobayashi, M.; Yamaguchi, R. *J. Am. Chem. Soc.* **2014**, *136*, 4829−4832. (c) Kawahara, R.; Fujita, K.-i.; Yamaguchi, R. *Angew. Chem., Int. Ed.* **2012**, *51*, 12790−12794. (d) Yamaguchi, R.; Ikeda, C.; Takahashi, Y.; Fujita, K.-i. *J. Am. Chem. Soc.* **2009**, *131*, 8410−8412.
(44) Siegl, W. O. *J. Org. Chem.* **1977**, *42*, 1872−1878.

DOI: 10.1021/acscatal.5b00952
ACS Catal. 2015, 5, 5468−5485